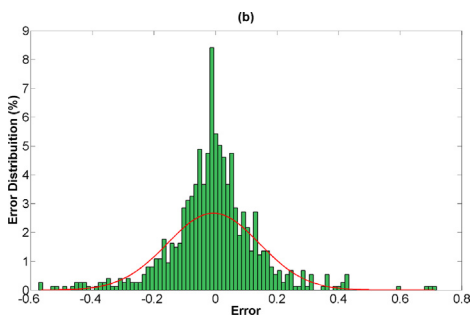




Full Length Article

Estimation of CO₂ equilibrium absorption in aqueous solutions of commonly used amines using different computational schemesAmir Dashti^{a,*}, Mojtaba Raji^b, Masood Sheikh Alivand^c, Amir H. Mohammadi^{d,e,*}^a Young Researchers and Elites Club, Science and Research Branch, Islamic Azad University, Tehran, Iran^b Separation Processes Research Group (SPRG), Department of Engineering, University of Kashan, Kashan, Iran^c Department of Chemical and Biomolecular Engineering, University of Melbourne, Australia^d Institut de Recherche en Génie Chimique et Pétrolier (IRGCP), Paris Cedex, France^e Discipline of Chemical Engineering, School of Engineering, University of KwaZulu-Natal, Howard College Campus, King George V Avenue, Durban 4041, South Africa

GRAPHICAL ABSTRACT



ARTICLE INFO

Keywords:
CO₂ capture
Absorption
Amine
CO₂ solubility
Modeling

ABSTRACT

In absorptive removal of CO₂ by aqueous alkanolamine solvent, as the most prevalent CO₂ capture technique, equilibrium absorption capacity of CO₂ is a significant parameter for assessing the efficiency of absorption systems. In this study, unique computational models are presented to estimate CO₂ solubility in commonly used amines. A series of models, including genetic algorithm-adaptive neuro fuzzy inference system (GA-ANFIS), particle swarm optimization ANFIS (PSO-ANFIS), coupled simulated annealing-least squares support vector machine (CSA-LSSVM) and radial basis function (RBF) neural networks were developed to estimate CO₂ equilibrium absorption capacity in twelve aqueous amine solutions. The model inputs comprise of CO₂ partial pressure, temperature, amine concentration in aqueous solution, molecular weight, hydrogen bond donor/acceptor count, rotatable bond count and complexity of the amines. The obtained results affirm that among proposed models, LSSVM exhibits more promising results with an excellent compatibility with experimental values. In detail, both mean square errors and average regression coefficient (R²) of LSSVM model are 0.02 and 0.9338, respectively. Moreover, it is confirmed that the proposed LSSVM model has better accuracy compared to the other models.

* Corresponding authors at: Institut de Recherche en Génie Chimique et Pétrolier (IRGCP), Paris Cedex, France (A.M. Mohammadi).

E-mail addresses: amirdashti13681990@gmail.com (A. Dashti), amir_h_mohammadi@yahoo.com (A.H. Mohammadi).

1. Introduction

Nowdays, reduction of CO₂ emission into the atmosphere is an important issue [1,2]. Among diverse greenhouse gases (GHGs), it is widely accepted that CO₂ is the most eminent GHG which leads to the nearly 60% of the global climate change [2,3]. Considering the before-mentioned implications of CO₂ emission, mainly released by CO₂ rich streams (e.g., flue gas), it is extremely important to remove CO₂ by efficient separation and purification techniques.

Absorption by using aqueous amine solvent is one of the most prevalent techniques for post-combustion CO₂ capture due to its privileges, such as high flexibility for industrial applications and great performance [4,5]. Among a wide variety of influential parameters in the absorptive removal of CO₂ by amine solvents, CO₂ solubility or equilibrium CO₂ capacity has been known as the most important parameter affecting the effectiveness and performance of amine solvents to a great extent [4].

Different separation and purification techniques have been extensively employed (e.g., physical and chemical absorption [5], cryogenic separation [6], adsorption by solid sorbents [7], membrane technology [8–10], and hybrid processes) for CO₂ capture from natural gas and post-combustion CO₂ capture. Although gas hydrates have attracted a great attention as a new technology [11,12], chemical absorption of CO₂ by alkanolamine solvents is the most preferred technique which has been used during past decades [13,14]. The physical and chemical properties of commercial amine solvents, mass transfer mechanisms and kinetics of absorption can be found in the published literature [15,16].

As well as typical measurements by experimental methods, a series of thermodynamic models have been proposed to calculate the equilibrium absorption capacity of CO₂ at various operating conditions. The well known thermodynamic models developed on the basis of vapor-liquid equilibrium (VLE) theory, include Kent-Eisenberg [17,18], electrolyte-NRTL [19], Deshmukh-Mather [20] and extended UNIQUAC [21,22]. Nevertheless, thermodynamic models are suffering from some drawbacks, which make them inappropriate for accurate estimation of CO₂ loading in a wide range of conditions and different amine solutions, and normally, physicochemical properties should be known for each amine solution. For instance, Benamor and Aroua [23] designed a number of experiments to assess the accuracy of modified Deshmukh-Mather model to estimate the CO₂ loading in DEA, MDEA and DEA/MDEA solutions at different operating temperatures (30–50 °C), CO₂ partial pressures (0.09–100 kPa) and amine concentrations (2–4 M). Though they reported an acceptable accuracy between experimental and model estimated values for both DEA and MDEA, the limited number of amines and narrow ranges of operating variables can seriously barricade its applicability.

Various methodologies of machine learning, including artificial neural network (ANN), adaptive neuro-fuzzy inference system (ANFIS) and support vector machine (SVM), have been presented for modeling and parametric estimation in different fields [24–26]. Similarly, many research works have investigated the application of machine learning methodologies in the area of aqueous alkanolamine solvents for CO₂ capture. Koolivand Salooki et al. [27] succeeded to estimate the output parameters of stripper column, located at Hashemi Nejad Gas Refinery in Iran, by using ANN model and reported a good agreement between operational data and the result obtained from model. Adib et al. investigated the ability of SVM model to estimate output variables of regeneration column (i.e., temperature and reflux flow rate) of Hashemi Nejad Gas Refinery [28]. A simple comparison between ANN and SVM model revealed that SVM can estimate processes variables better than ANN model with minimum square correlation coefficient of 0.99. In 2014, Ghiasi and Mohammadi [29] utilized Least Squares Support Vector Machine (LSSVM) approach to model CO₂ loading in different aqueous amine solvents with different concentrations, temperatures and CO₂ partial pressures. In 2016, Ghiasi et al. [1] employed ANFIS

technique to model a similar system and indicated that ANFIS soft computing approach substantially improves the accuracy of model to estimate the process variables, compared to the previously used LSSVM.

Saghatoleslami and his colleagues [30] performed similar experiments by genetic algorithm. Sipöcz et al. [31] used feed forward ANN to model steady-state CO₂ capture process by aqueous MEA solvent in a power plant. In the published article by Zhou et al. [32], a combination of ANN with both adaptive-network-based fuzzy interface system (ANFIS) and sensitivity analysis was used to model post-combustion CO₂ capture by amine solvents. Similar investigations can be found in the published research works [33–35].

ANN modeling was employed to estimate the experimental values of CO₂ solubility in aqueous TIPA, TIPA/MEA and TIPA/PZ solutions by Daneshvar et al. [36]. Shahsavand and his coworkers [37] studied the capability of both radial basis function neural network and multi-layer perceptron ANN to calculate the equilibrium CO₂ absorption capacity of aqueous DEA and MDEA solutions considering different concentrations and rates. A comparative study was performed by Pahlavanzadeh et al. [38] to evaluate the abilities of Deshmukh-Mather and ANN models to estimate CO₂ solubility in 2-amino-2-methyl-1-propanol (AMP) at low partial pressures (7.47–69.87 kPa). ZareNezhad and Aminian used a feed-forward ANN model to estimate the H₂S solubility in PZ solvent [39] and a fuzzy network model to anticipate the solubility of H₂S in aqueous brine solutions [40]. In another research, Bastani et al. [41] employed feed forward ANN model to estimate CO₂ absorption capacity of aqueous chemical absorbers in a wide range of operating parameters (i.e., temperature, pressure and concentration).

To the best of our knowledge, there is not any research work attempting to estimate the experimentally obtained values of CO₂ absorption capacities of all kinds of aqueous amines by only a single comprehensive model.

In this work, the experimental data of CO₂ solubility in three commercialized amines (including MEA, DEA, and MDEA) and nine recently developed amines (including 2-amino-2-methyl-1-propanol (AMP), piperazine (PZ), triisopropanolamine (TIPA), mono-propanolamine(MPA), 1-amino-2-propanol (MIPA), 4-(diethylamino)-2-butanol(DEAB), methyl amino ethanol (MAE), 2-(Diethylamino)-ethanol(DEEA) and 3-(Methylamino)-propylamine (MAPA)) were used which can cover primary, secondary and tertiary amine classification. Hence, the accurate results of ANN models for anticipating the equilibrium CO₂ absorption capacities of all before-mentioned amine solutions can ameliorate the limitations of typical theoretical models, which are only applicable for specific cases.

Almost all previously published research papers agree that data validation is the most crucial factor for developing a promising model.

2. Methodology

2.1. Radial basis function neural network (RBF-NN)

RBF-ANN is constructed from three layers; namely input, output and hidden layers [42]. Among different ANNs, RBF-ANN can be categorized into the single hidden layer group which is more beneficial than multiple interconnected hidden layers, such as the multilayer perception neural network (MLP-NN) [42]. In detail, activation function and the maximum number of neurons are two important parts of RBF-NN, which can substantially affect the processing conditions. Gaussian function is normally used as the most popular activation function in the hidden layer of RBF-NNs, which has smoother behavior compared to the other types of MF. The Gaussian function as a radial function can be represented as follows:

$$\phi(r) = \exp\left(-\frac{(x - c)^2}{r^2}\right) \quad (1)$$

where ϕ is activation function; the center (c) and radius (r) are the

Table 1

Details of the data used in the modeling.

Pressure (kPa)	Temperature (K)	Molarity (mol/lit)	Molecular Weight	HBDC	HBAC	RBC	COMPLEXITY	Number of data	Sample	References
3.2–94	303–323	2–3.4	89.13624	2	2	1	42.8	51	AMP	[74]
0.032–1487	298–343	0.2–4.5	86.14	2	2	0	26.5	390	PZ	[75–77]
0.00144–6000	298.15–393.15	0.183617–5	61.084	2	2	1	10	237	MEA	[78–89]
0–6165.793	283–422	0.47792–4.28	119.164	2	3	4	43.7	731	MDEA	[79,80,82,90–101]
0.0129–7017	388.75–339.81	0.057455–4	105.137	3	3	4	28.9	542	DEA	[79,81,82,98,102–104]
1.264–153.4	298.15–353.2	0.5–5	101.193	0	1	3	25.7	63	TEA	[105,106]
9–100	298–333	1–5	145.246	1	2	5	71.7	60	DEAB	[107]
0.6–577.1	313.15–393.15	5	117.192	1	2	4	43.8	91	DEEA	[108]
0.9–355.9	303.1–323.1	1–4	75.111	2	2	4	16.4	73	MAE	[109]
0.3–534.5	313.15–393.15	1–2	88.15	2	2	3	21.5	94	MAPA	[108]
2.5–704.9	313.15–393.15	2–5	75.11	2	2	2	16.4	101	MPA	[110]
10.73–78.42	303.15–343.15	2	191.271	3	4	6	108	25	TIPA	[36]

HBDC = Hydrogen Bond Donor Count, HBAC = Hydrogen Bond Acceptor Count, RBC = Rotatable Bond Count.

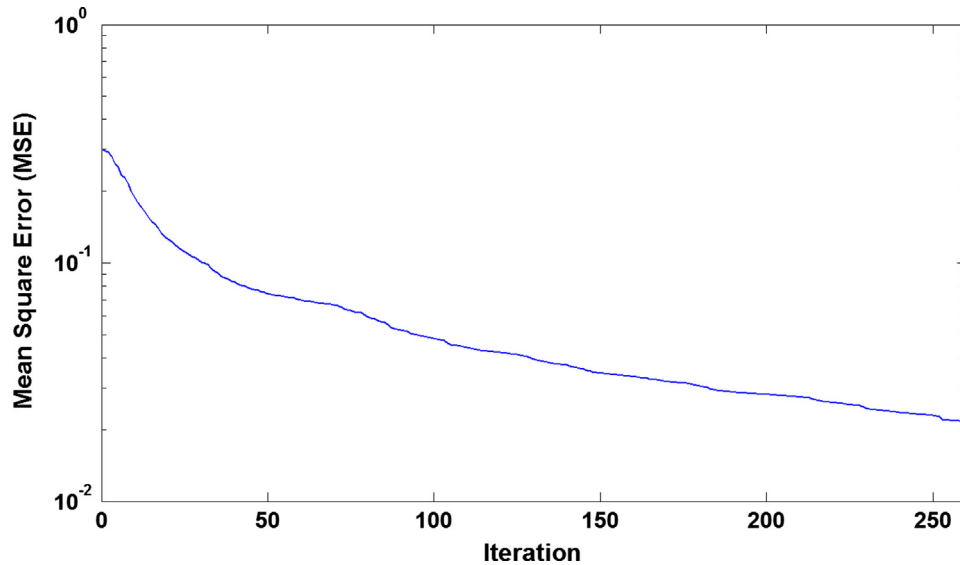


Fig. 1. Variations of MSE in different iterations for RBF-ANN model.

Table 2Properties of the PSO-ANFIS model for estimating CO₂ solubility in amines.

Parameter	Value
Iterations	400
No. of particles	4000
Initial inertia weight (W_{\min})	0.5
Inertia Weight Damping Ratio (W_{damp})	0.99
Cognitive acceleration (C_1)	1
Social acceleration (C_2)	2
No. of fuzzy rules	10

variable of Gaussian RBF. Additionally, a multi quadric RBF is denoted as follow:

$$\phi(r) = \frac{\sqrt{r^2 + (x - c)^2}}{r} \quad (2)$$

In addition, RBF-NNs use a comprehensive procedure to evaluate the optimum values, which makes them a powerful tool for interpolation of the data [43].

Gaussian-like RBFs are local and more commonly employed than multi quadric RBFs. They may be applied in any type of linear and nonlinear models and any type of single or multi-layer networks. Nevertheless, based on the study performed by Broomhead and Lowe [44], RBF networks have been associated with radial functions in a single layer network [45].

Table 3Properties of the GA-ANFIS model for estimating CO₂ solubility in amines.

Parameter	Value
No. of population	400
No. of generation	4000
Mutation (%)	90
Crossover (%)	65
Selection Pressure	8
Mutation Rate (%)	5
No. of fuzzy rules	10

2.2. Adaptive neuro fuzzy inference system

The Fuzzy Logic (FL) was first introduced by Lotfi Zadeh [46] in 1965 which was surprisingly able to connect linguistic variables to their corresponding mathematical formats. As a result, FL can qualitatively evaluate a system and gain particular data in comparison to the conventional numerical methods. Nevertheless, FL fails to accurately model different systems and the results are not satisfactory most of the times. This problem can be ascribed to the hesitation and/or conflict in making decision which can be easily found among scientists and specialists [43]. To overcome this challenge, the special features of FL should be combined with other quantitative methods like ANNs, which are so fast in data acquisition and leaning from extracted information [114]. The coupled strategy utilizing both FL and ANN approaches is

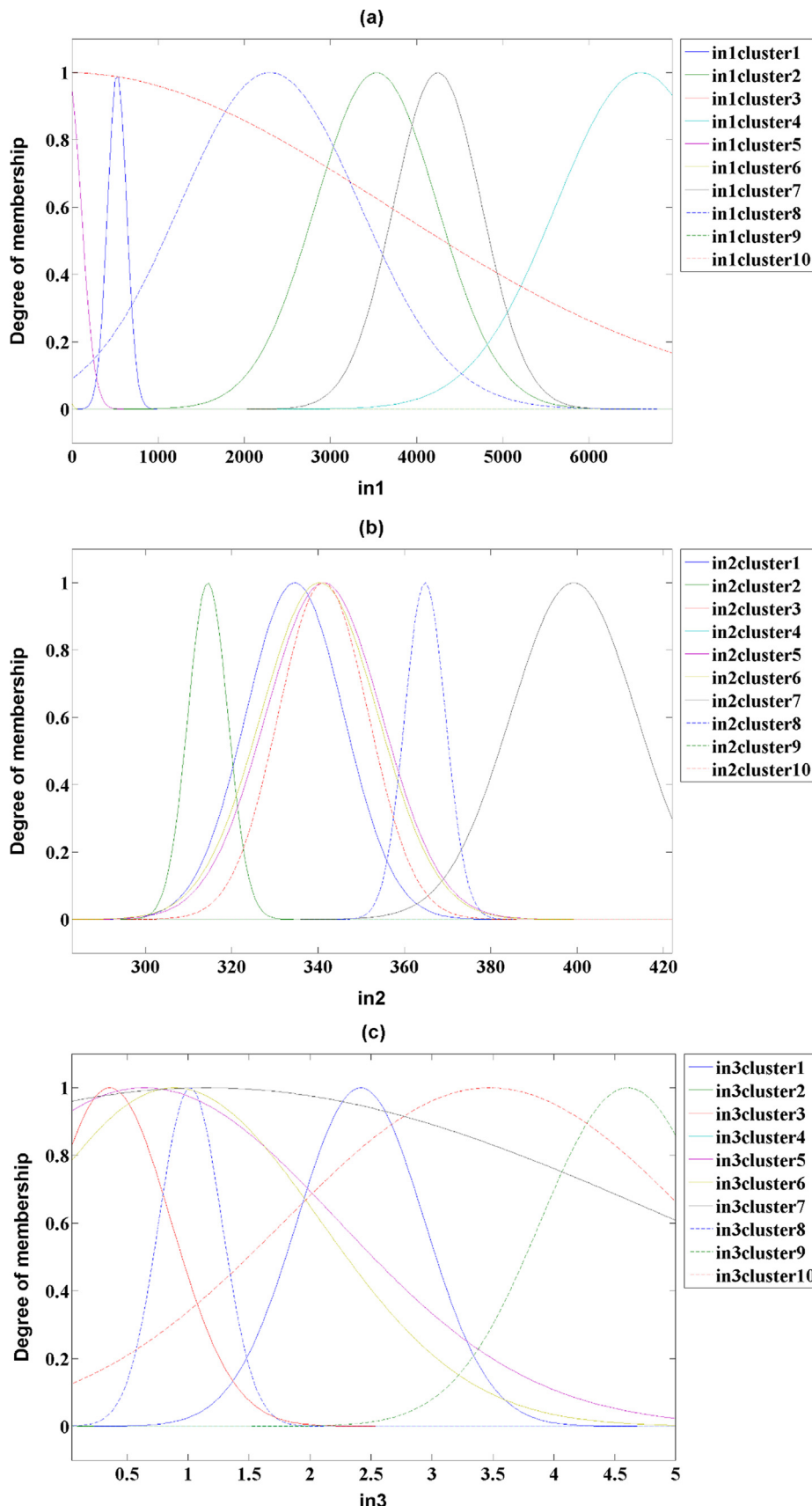


Fig. 2. Corresponding membership functions of PSO-ANFIS for different input terms: (a) pressure, (b) temperature, (c) molarity, (d) molecular weight, (e) hydrogen bond donor count, (f) hydrogen bond acceptor count, (g) rotatable bond count and (h) complexity.

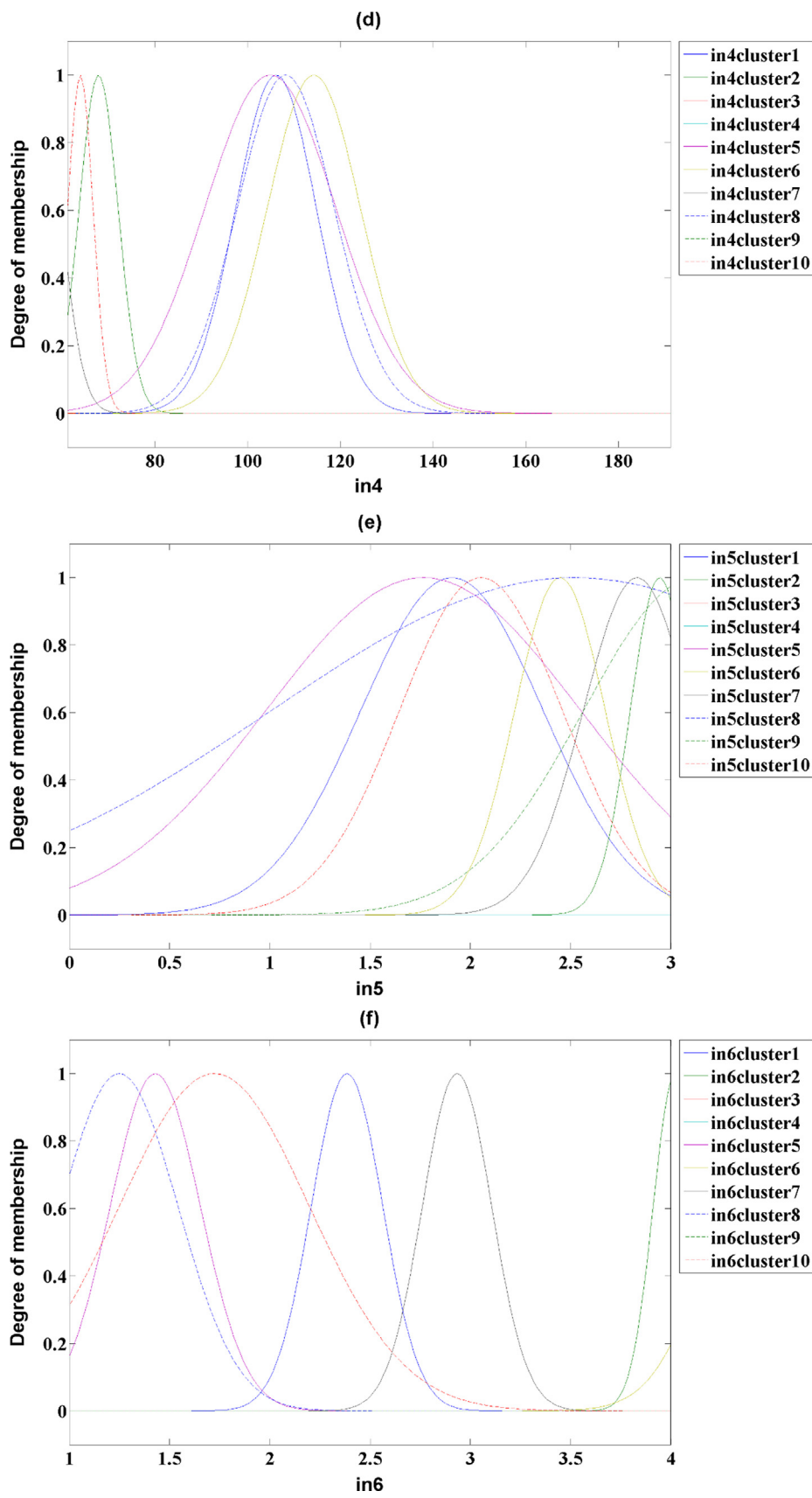


Fig. 2. (continued)

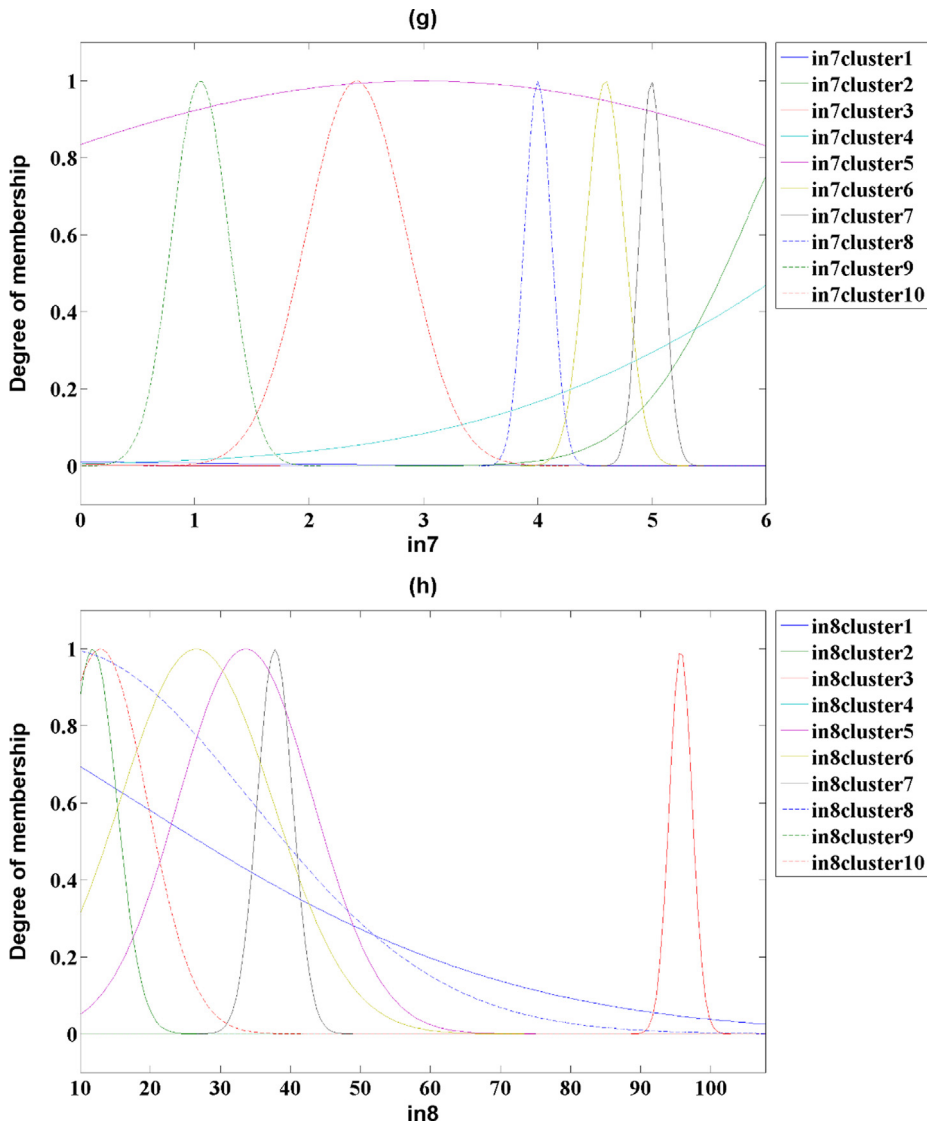


Fig. 2. (continued)

called Adaptive Neuro-Fuzzy Interface System (ANFIS). The connection process is normally implemented by employing membership functions (MFs) and Fuzzy Interface System (FIS), which can significantly control the modeling process [114,48]. On the basis of previously published papers, Mamdani and TSK are two accessible types of FIS which both work with intellectual if-then rules. As it was reported, both sorts of FISs have their own advantageous and drawbacks. However, as better precession, certainty and nonlinearity handling have been reported for TSK type [48], herein TSK was chosen as a proper kind of FIS to tackle the existing nonlinearity input and output vectors. A simple ANFIS structure has input (i.e., X_1 and X_2) and output (i.e., Y) parameters. The role of if-then rules for TSK FIS structure is presented below [114] :

$$\begin{aligned} \text{If } (X_1 \text{ is } A_1 \text{ and } X_2 \text{ is } B_2) \text{ Then } & (f_1 = m_1 X_1 + n_1 X_2 + r_1) \\ \text{If } (X_1 \text{ is } A_2 \text{ and } X_2 \text{ is } B_2) \text{ Then } & (f_2 = m_2 X_1 + n_2 X_2 + r_2) \\ \text{If } (X_1 \text{ is } A_1 \text{ and } X_2 \text{ is } B_2) \text{ Then } & (f_3 = m_3 X_1 + n_3 X_2 + r_3) \\ \text{If } (X_1 \text{ is } A_2 \text{ and } X_2 \text{ is } B_1) \text{ Then } & (f_4 = m_4 X_1 + n_4 X_2 + r_4) \end{aligned} \quad (3)$$

where A_i and B_i are correspondingly fuzzy sets of input parameters; m_i , n_i and r_i are the coefficients of output parameters. It should be noted that the expressions after *If* and *Then* are respectively denoted as antecedent and consequences.

The typical ANFIS structure is composed of five layers, which are expressed in detail as following [43]:

Layer 1:

The main responsibility of this layer is the conversion of unprocessed input data to linguistic terms. In this layer, linguistic terms should be defined on the basis of a suitable MF (e.g., Gaussian) to import input X_1 and X_2 parameters to the nodes of this layer. The Gaussian MF used in this study is given by the following mathematical framework:

$$O_i^1 = \beta(X) = \exp\left(-\frac{1}{2} \frac{(X - Z)^2}{\sigma^2}\right) \quad (4)$$

where the layers output is denoted by O , σ is variance term and Z is the center point of Gaussian MF.

Layer 2:

The second layer or firing strength layer determines the sufficiency of applied conditions and is mainly responsible for the accuracy of calculations. The used formula is given as below:

$$O_i^2 = W_i = \beta_{Ai}(X) \cdot \beta_{Bi}(X) \quad (5)$$

Layer 3:

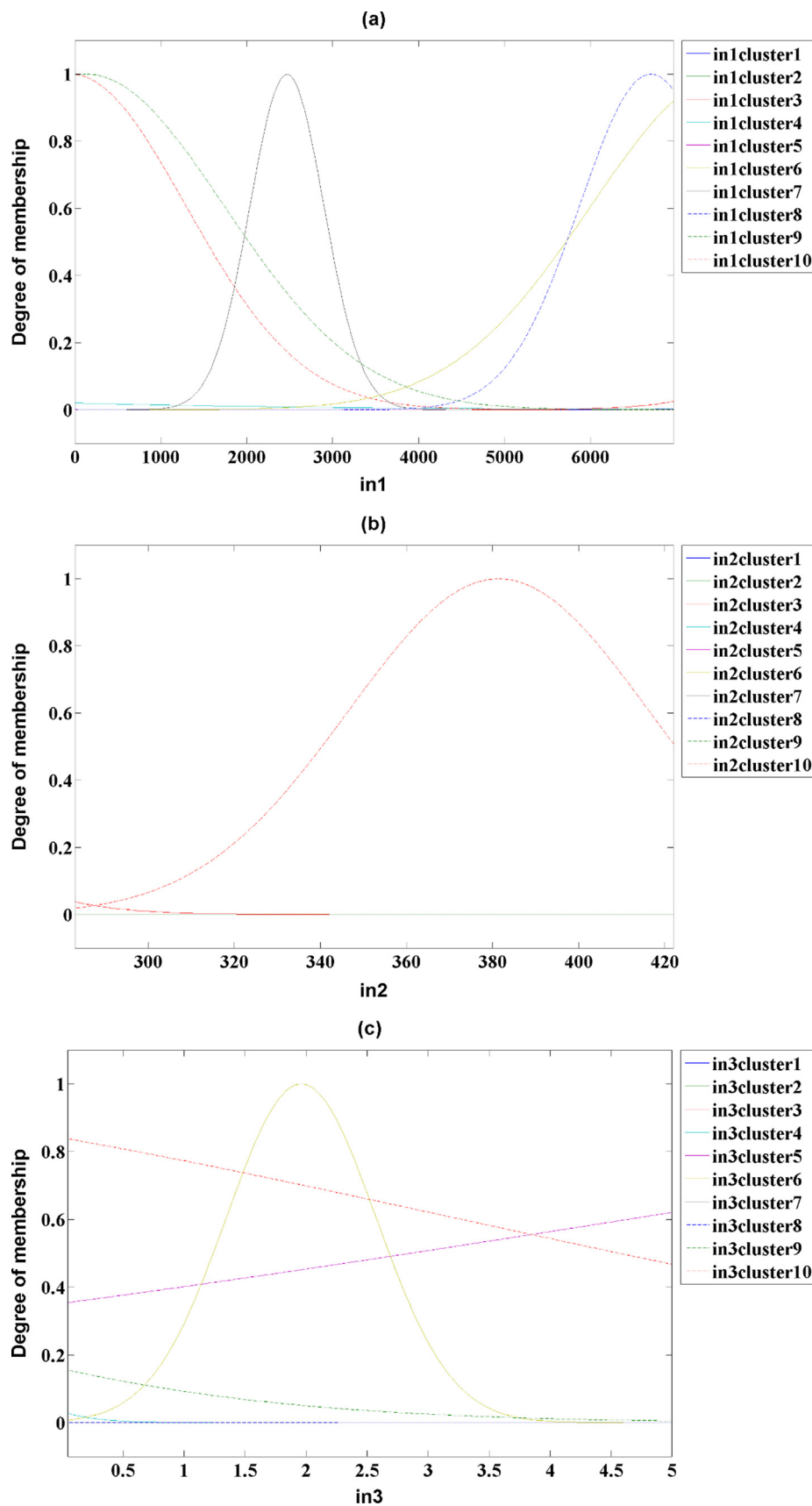


Fig. 3. Corresponding membership functions of GA-ANFIS for different input terms: (a) pressure, (b) temperature, (c) molarity, (d) molecular weight, (e) hydrogen bond donor count, (f) hydrogen bond acceptor count, (g) rotatable bond count and (h) complexity.

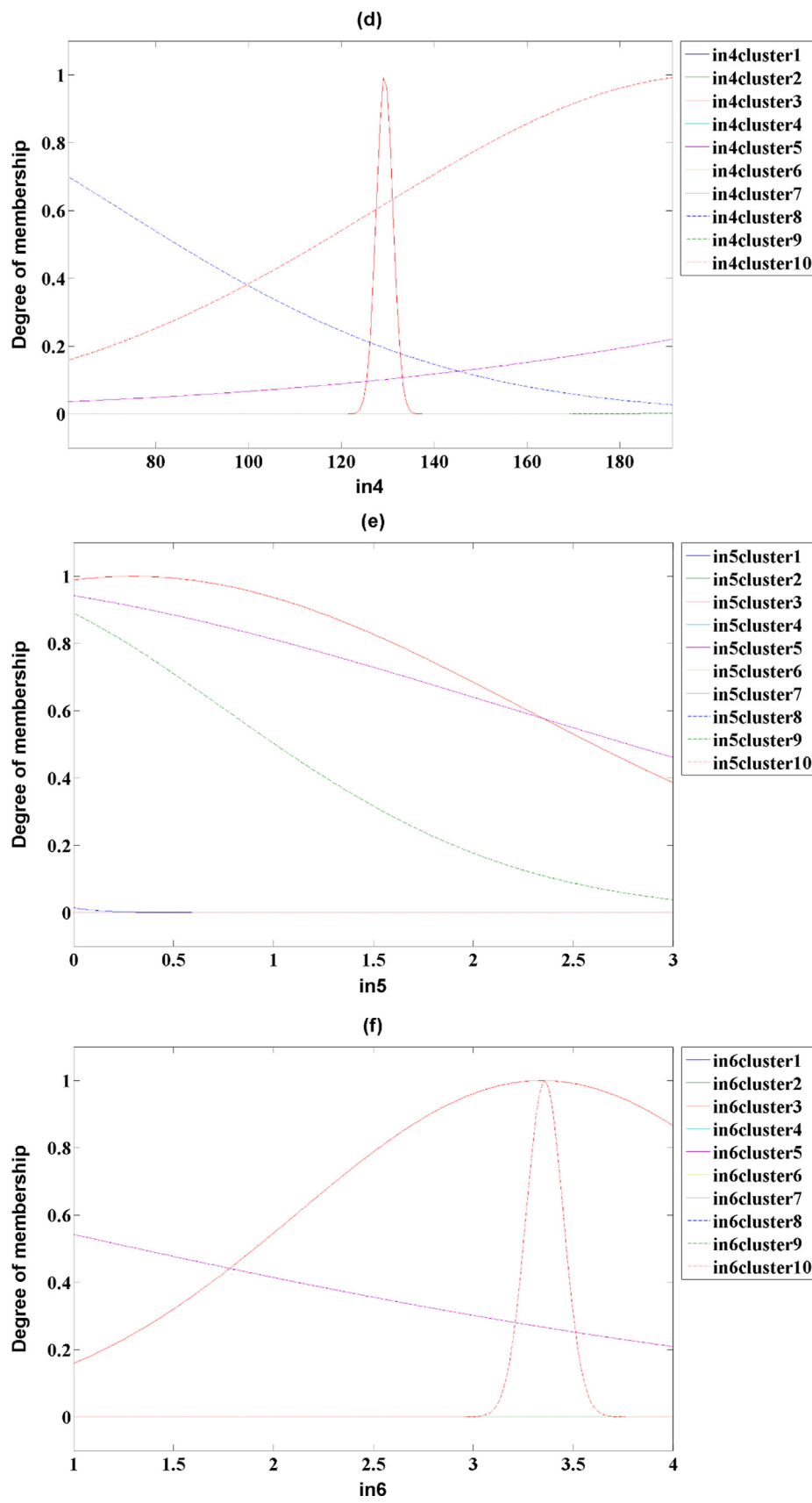


Fig. 3. (continued)

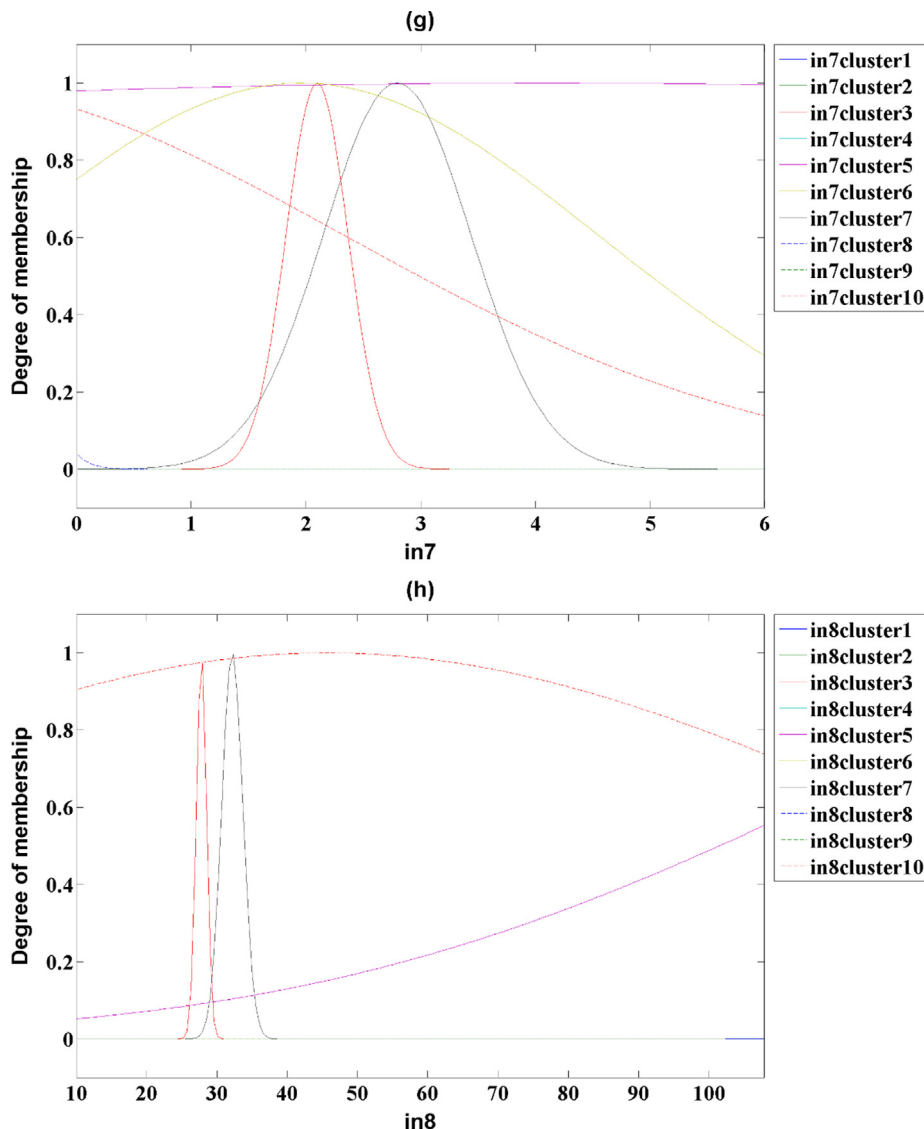


Fig. 3. (continued)

The calculated W_i values in the second layer should be normalized in the third layer which can differentiate among firing strength of rules as:

$$O_i^3 = \frac{W_i}{\sum_i W_i} \quad (6)$$

Layer 4:

In this layer, the linguistic terms of output are assessed considering the effect of each single node on the models output. The used formulation in this layer is expressed as follow:

$$O_i^4 = \bar{W}_i f_i = \bar{W}_i (m_i X_1 + n_i X_2 + r_i) \quad (7)$$

where m_i , n_i and r_i denote the linear variables of model. To provide a better consistency between model estimated results and experimentally obtained values, the before mentioned variables (i.e., m_i , n_i and r_i) and the variables of first layer should be optimized by ANFIS model.

Layer 5:

This layer is responsible to sum up all incoming signals and compute the total output values by employing weighted average sum method as

below:

$$O_i^5 = Y = \sum_i W_i f_i = \bar{W}_1 f_1 + \bar{W}_2 f_2 = \frac{\sum_i W_i f_i}{\sum_i W_i} \quad (8)$$

2.3. Particle swarm optimization (PSO)

PSO is a well-known optimization technique, which was first introduced in 1995 by inspiration of natural population patterns, which can be easily found in the nature [50,51]. In the PSO algorithm, particles are defined as the solutions of a specific problem and swarm represents the group of particles. Hence, particle and swarm are respectively the representative of individual and population, which are used in other optimization algorithms, such as Genetic Algorithm (GA) [115].

In PSO approach, particles chase optimum particles in the domain space by evaluating the success of neighborhood (e.g., physical, social and queen [53]) and the generations are updated on the basis of initial population in order to reach the optimum solution [54]. Particles can be identified by their own position (x_i) and velocity (v_i) vectors. The velocity vector of particles at each time interval can be calculated by the following mathematical formula [55–57]:

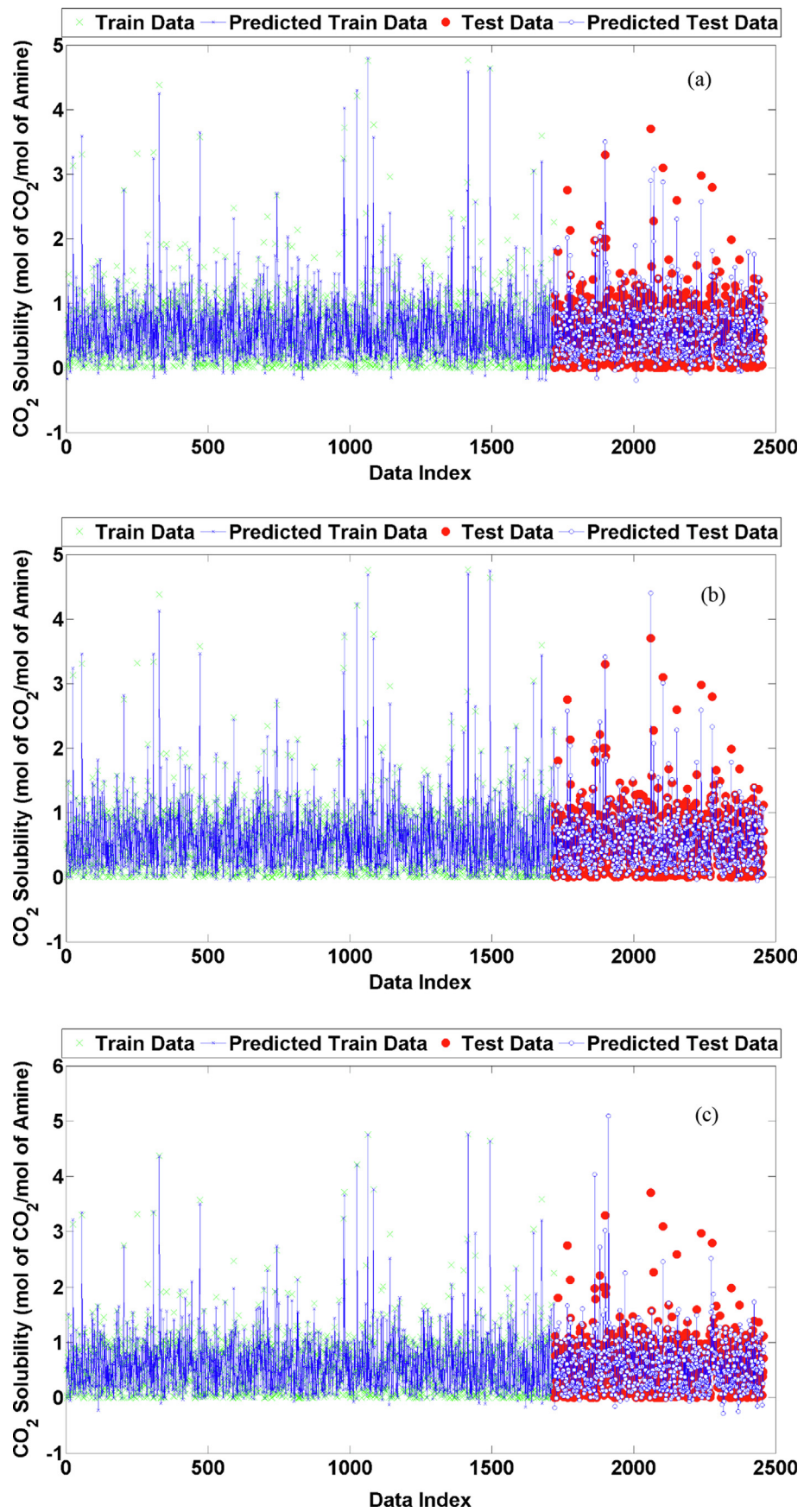


Fig. 4. Experimental and estimated values for various models against data index: (a) PSOANFIS, (b) LSSVM, (c) RBF and (d) GAANFIS.

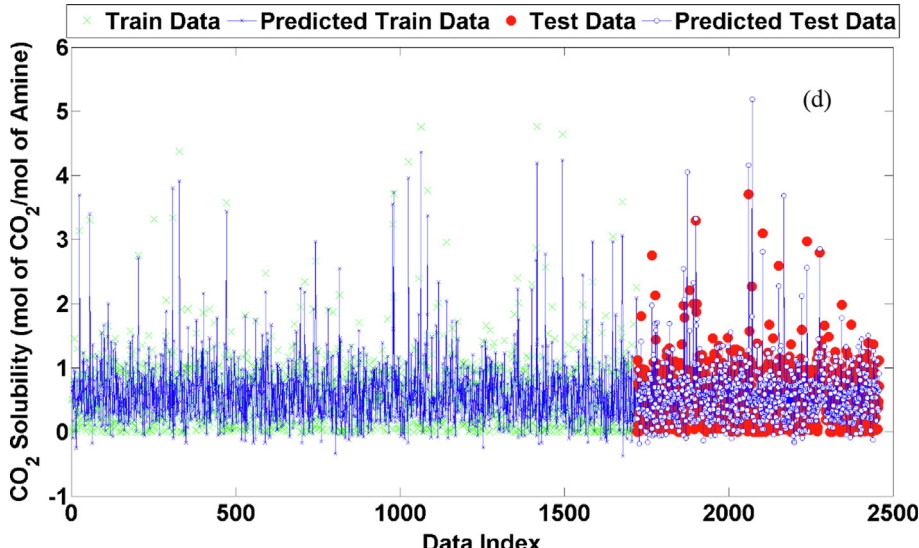


Fig. 4. (continued)

$$\begin{aligned} v_{id}(t+1) &= wv_{id}(t) + c_1 r_1 (P_{best,id}(t) - x_{id}(t)) + c_2 r_2 (g_{best,d}(t) - x_{id}(t)), \\ d &= 1, 2, \dots, D \end{aligned} \quad (9)$$

where $P_{best, id}$ is the optimum position of particle i obtained in the previous step; $g_{best, d}$ is the optimum global position; w is inertia weight factor; c_i ($i = 1, 2$) is learning rate; r_i ($i = 1, 2$) is random coefficient with a value between 0 and 1 [58]. The abovementioned equation is composed of three main parts, namely, inertia, cognitive and social [50,55,59,60]. The inertia part ($wv_{id}(t)$) is responsible to memorize the direction of particles during movement through their paths. The second term or cognitive component provides a velocity term by pushing particles toward the prior optimum positions. The third or social term assesses the efficiency of particles compared to their neighbors and moves the swarms in the domain space. The position of particles at $(t+1)$ time interval can be calculated by summing up the novel particle velocity to the prior positions at t :

$$x_{id}(t+1) = x_{id}(t) + v_{id}(t+1), \quad d = 1, 2, \dots, D \quad (10)$$

2.4. LSSVM

Support Vector Machine (SVM) is an accurate machine learning methodology which works on according to the statistical learning theory [61–63]. Among a wide range of applications, this method has been studied for regression analysis due to its advantageous, such as high flexibility and having low tuning variables [63–66].

The SVM technique constructs a distinct hyper surface in the input space. This procedure is accomplished in the following way [61,67,68]: 1) It maps the input patterns into an elevated dimensional feature space via nonlinear mapping. 2) Construct a distinct hyper-plane with the highest margin. We assume having training samples $((x_1, y_1), (x_2, y_2), \dots, (x_n, y_n))$ with input data $x_i \in R^n$ and output data $y_i \in R$ with class labels $-1, 1$ for classes 1 and 2, respectively. If the aforementioned data sample is linearly distinct in the feature space, then the SVM estimates the function by the following relationship [61,68]:

$$y = \omega^T \phi(x) + b \quad (11)$$

where x is model input; $\phi(x)$ is the nonlinear kernel function mapping x from lower dimensions into n -dimensional space; ω^T is the transposed output layer vector and b is bias term. If the data of classes can be distinguished, it can be written that [61,68]:

$$\begin{cases} \omega^T \phi(x_k) + b \geq +1, & \text{if } y_k = +1 \\ \omega^T \phi(x_k) + b \leq +1, & \text{if } y_k = -1 \end{cases} \quad (12)$$

The above equation can be rewritten as [61,68]:

$$y_k [\omega^T \phi(x_k) + b] \geq +1, \quad k = 1, 2, \dots, N \quad (13)$$

The extension of linear SVMs to non-separable case was proposed by Cortes and Vapnik. By adding some slack variables, the above equation is converted as follow [62]:

$$y_k [\omega^T \phi(x_k) + b] \geq +1 - \xi_k, \quad k = 1, 2, \dots, N \quad \xi_k \geq 0 \text{ for } k = 1, \dots, N \quad (14)$$

The generalized optimal separating hyper-plane is determined by the vector w that minimizes the functional [61,68]:

$$\phi(\omega, \xi) = \frac{1}{2} \omega^T \omega + \frac{C}{2} \sum_{i=1}^N \xi_i^p \quad (15)$$

with the following constraint:

$$\text{while: } y_k [\omega^T \phi(x_k) + b] \geq +1 - \xi_k, \quad k = 1, 2, \dots, N \quad (16)$$

where C is real constant ($C > 0$) that is obligated to control the tradeoff between the highest margin and the least classification error [67–69]. In the SVM algorithm, optimum separating hyper-plane is acquired by solving the quadratic programming problem of the Eq. (15). The solution of Eq. (15) under the constraints of is given by the saddle point of the Lagrangian [70]:

$$\begin{aligned} \phi(\omega, b, \alpha, \xi, \beta) &= \frac{1}{2} \omega^T \omega + \frac{C}{2} \sum_{i=1}^N \xi_i - \sum_{i=1}^N \alpha_i (y_i [\omega^T x_i + b] - 1 + \xi_i) - \sum_{i=1}^N \beta_i \xi_i \end{aligned} \quad (17)$$

where α, β is Lagrangian multiplier [61,68]. Suykens and Vandewalle [61] succeeded to modify the conventional version of SVM and develop least squares SVM (LSSVM) as a superior version of SVM. The LSSVM reduces the complexity of SVM model by solving linear equations instead of finding the solution for a set of complicated quadratic programming equations [63–65]. The LSSVM method is trained by minimizing the cost function that is defined as follows [61,68]:

$$\phi(\omega, \xi) = \frac{1}{2} \omega^T \omega + \frac{C}{2} \sum_{i=1}^N \xi_i^2 \quad (18)$$

With the following equality constraints:

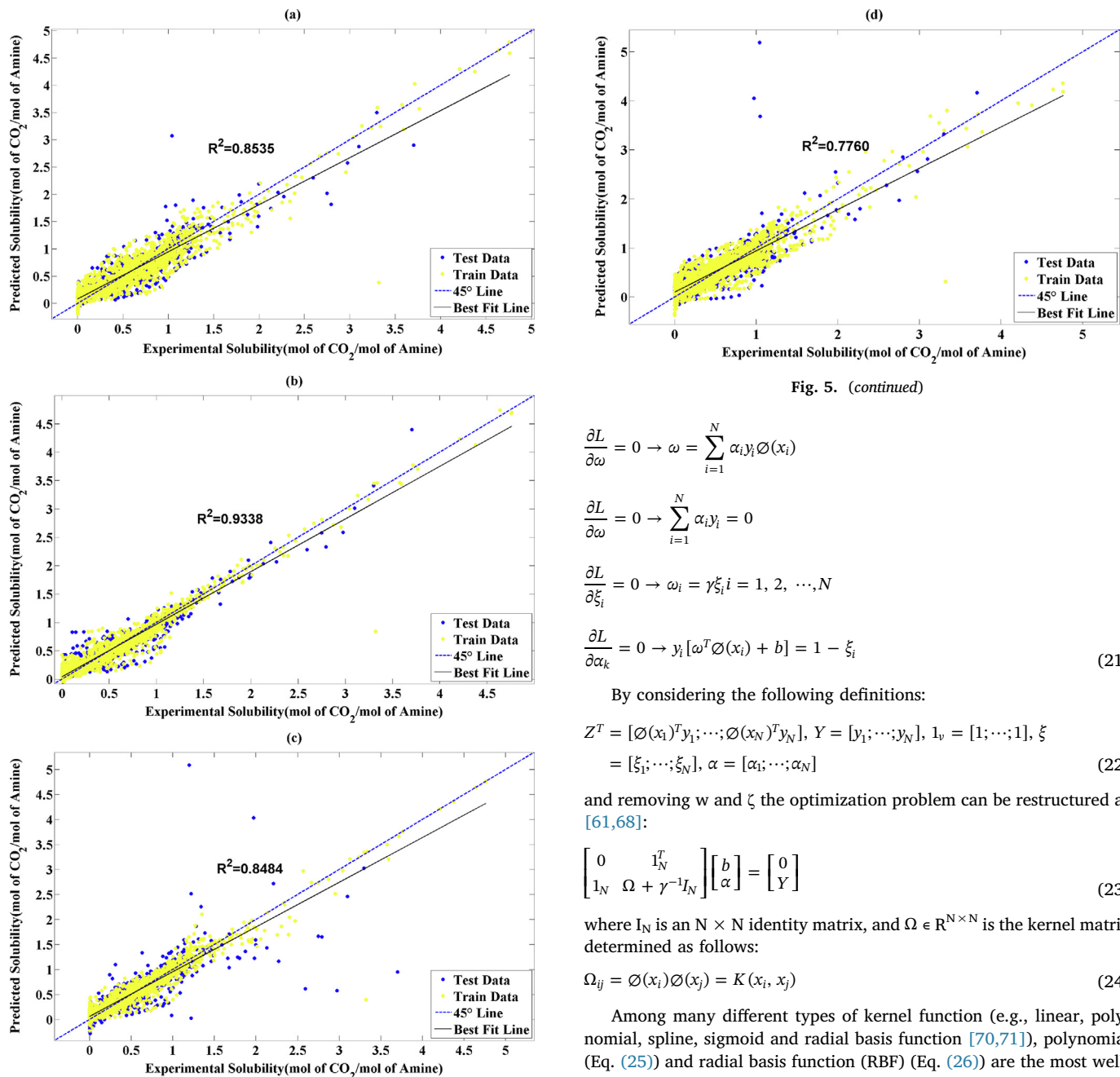


Fig. 5. Comparison of the experimental data of CO₂ solubility in various Amines and the estimated values obtained for different models: (a) PSOANFIS, (b) LSSVM, (c) RBF and GAANFIS.

$$y_i [\omega^T \phi(x_i) + b] = 1 - \xi_i, i = 1, 2, \dots, N \quad (19)$$

According to Eq. (19), in the LSSVM the inequality constraints have been substituted by equality constraints, which leads to solving of linear equations and faster calculation time.

The Lagrange function is normally utilized for handling LSSVM nonlinear classification problems [61,68]:

$$L(\omega, b, \xi, \alpha) = \frac{1}{2} \omega^T \omega + \frac{C}{2} \sum_{i=1}^N \xi_i^2 - \sum_{i=1}^N \alpha_i \{y_i [\omega^T \phi(x_i) + b] - 1 + \xi_i\} \quad (20)$$

where α_i values are Lagrange multipliers. To save the optimality of function yield, the following equations should be applied [68,69]:

$$\begin{aligned} \frac{\partial L}{\partial \omega} &= 0 \rightarrow \omega = \sum_{i=1}^N \alpha_i y_i \phi(x_i) \\ \frac{\partial L}{\partial \omega} &= 0 \rightarrow \sum_{i=1}^N \alpha_i y_i = 0 \\ \frac{\partial L}{\partial \xi_i} &= 0 \rightarrow \omega_i = \gamma \xi_i, i = 1, 2, \dots, N \\ \frac{\partial L}{\partial \alpha_k} &= 0 \rightarrow y_i [\omega^T \phi(x_i) + b] = 1 - \xi_i \end{aligned} \quad (21)$$

By considering the following definitions:

$$\begin{aligned} Z^T &= [\phi(x_1)^T y_1; \dots; \phi(x_N)^T y_N], Y = [y_1; \dots; y_N], 1_v = [1; \dots; 1], \xi \\ &= [\xi_1; \dots; \xi_N], \alpha = [\alpha_1; \dots; \alpha_N] \end{aligned} \quad (22)$$

and removing w and ζ the optimization problem can be restructured as [61,68]:

$$\begin{bmatrix} 0 & 1_N^T \\ 1_N & \Omega + \gamma^{-1} I_N \end{bmatrix} \begin{bmatrix} b \\ \alpha \end{bmatrix} = \begin{bmatrix} 0 \\ Y \end{bmatrix} \quad (23)$$

where I_N is an $N \times N$ identity matrix, and $\Omega \in \mathbb{R}^{N \times N}$ is the kernel matrix determined as follows:

$$\Omega_{ij} = \phi(x_i) \phi(x_j) = K(x_i, x_j) \quad (24)$$

Among many different types of kernel function (e.g., linear, polynomial, spline, sigmoid and radial basis function [70,71]), polynomial (Eq. (25)) and radial basis function (RBF) (Eq. (26)) are the most well-known kernel functions, which are preferably used for LSSVM:

$$K(x_i, x_j) = (1 + \frac{x_i^T x_j}{c})^d \quad (25)$$

$$K(x_i, x_j) = \exp\left(-\frac{\|x_i - x_j\|^2}{\sigma^2}\right) \quad (26)$$

where σ^2 is tuning parameter of the Gaussian function; d denotes the degree of polynomial. In this work, RBF kernel was used like many other researches.

2.5. Coupled simulated annealing (CSA)

The CSA (proposed by Suykens and Vandewalle [69]) is a modified class of simple Simulated Annealing (SA), containing a series of parallel SA with higher accuracy and comparable convergence speed [72]. Moving toward solutions with worse quality and escaping from local optima are the main drawbacks of SA, which have been ameliorated in the CSA version. Therefore, the CSA can escape from local optimum in

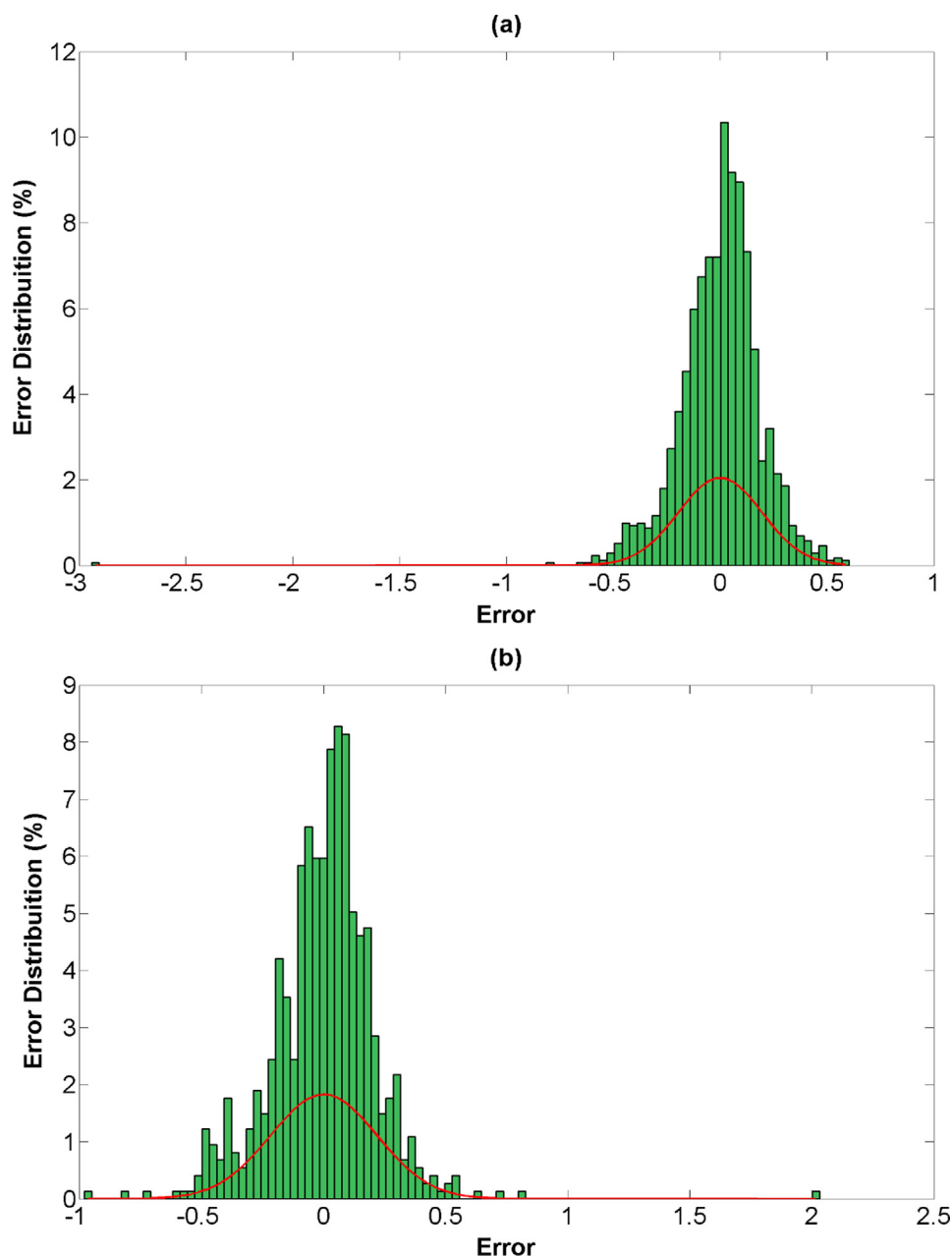


Fig. 6. Errors histogram for foreseeing the CO₂ solubility in various amines by PSOANFIS: (a) training dataset and (b) testing dataset.

non-convex problems, exhibit better calculation accuracy, higher acceptance probability, while maintaining the convergence speed during the optimization of problem [73]. Herein, MLP parameters were optimized by RB, LM, BR and SCG, LSSVM optimization was done by applying CSA and RBF optimization was carried out by GAS/PSO.

3. Data acquisition

3.1. General step

In order to employ machine learning technique for modeling CO₂ solubility in diverse aqueous amine solutions (e.g., MEA, DEA, and MDEA, AMP, PZ, TIPA, MPA, MIPA, DEAB, MAE, DEEA and MAPA), a comprehensive databank of experimental data was extracted from literature. The CO₂ solubility is defined as the moles of CO₂ per moles of amine and is a function of CO₂ partial pressure (P_{CO₂}, kPa), temperature (T, K), amine concentration (C_{amine}, mol/L), molecular weight

hydrogen bond donor/acceptor count, rotatable bond count and complexity of the amines. Molecular weight, hydrogen bond donor/acceptor count, rotatable bond count and complexity of the amines were obtained from the PubChem website.

The detailed conditions for absorptive CO₂ capture in the amine solvents, including partial pressure, temperature, amine concentration and CO₂ loading, are listed in Table 1, which also specify as independent variables in the model. During the computation, the whole available data points were divided into two categories; training set and testing set. The training data (75% of the whole data set) were applied for training process and model development and the remained 25% of total data points were employed for testing phase.

The efficiency, performance and accuracy of the used models to estimate experimental values were evaluated by the square of correlation coefficient (R²), mean relative error (MRE), mean absolute error (MAE), mean square error (MSE) and standard deviation (STD), all formulated in the below mentioned equations:

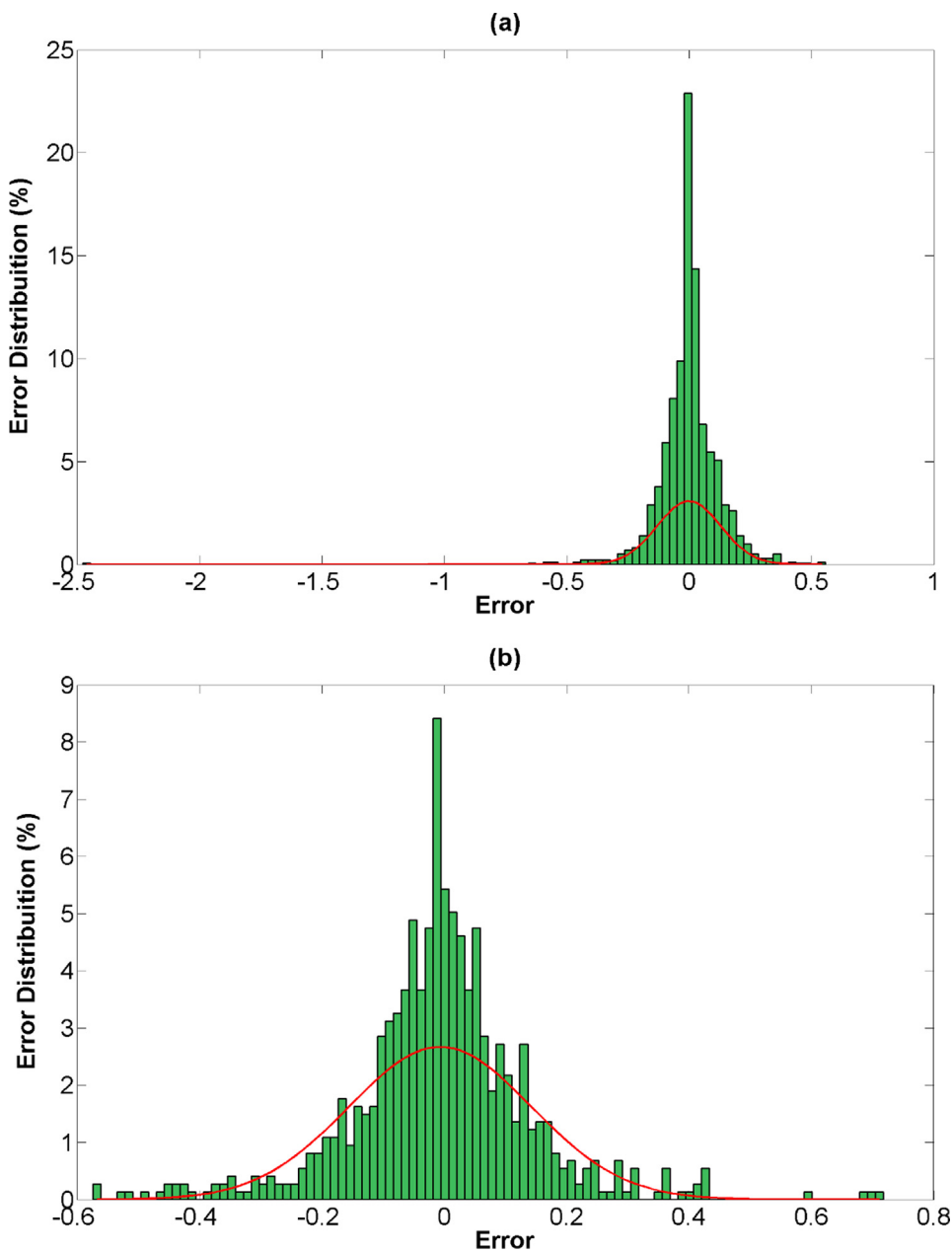


Fig. 7. Errors histogram for foreseeing the CO₂ solubility in various amines by LSSVM: (a) training dataset and (b) testing dataset.

$$R^2 = 1 - \frac{\sum_{i=1}^n [x_i^{sim} - x_i^{exp}]^2}{\sum_{i=1}^n [x_i^{sim} - x_m]^2}, \quad x_m = \frac{\sum_{i=1}^n x_i^{exp}}{n} \quad (27)$$

$$MRE = \frac{1}{n} \sum_{i=1}^n \frac{|x_i^{sim} - x_i^{exp}|}{x_i^{exp}} \quad (28)$$

$$MSE = \frac{1}{n} \sum_{i=1}^n (x_i^{exp} - x_i^{sim})^2 \quad (29)$$

$$MAE = \frac{1}{N} \sum_N |x^{sim} - x^{exp}| \quad (30)$$

$$STD = \sqrt{\sum_{i=1}^n \left(\frac{(x_i^{sim} - x_m)^2}{n} \right)^{0.5}} \quad (31)$$

where x^{sim} and x^{exp} represents prognosticated and experimental data, respectively and n is number of data points.

4. Results and discussion

4.1. Model development

The CSA approach was utilized to find the optimal values of the LSSVM parameters, including γ and σ^2 . Values of these parameters are 101.6330 and 0.389, respectively. The structure of RBF consists of couple of tuning parameters that are maximum number of neurons and spread. The trial and error were employed to find the optimum values, which were 95 and 260, respectively. The MSE values at different neurons are depicted in Fig. 1. PSO and GA methods were employed to determine optimum values of ANFIS parameters and train ANFIS model, which are necessary pre-steps for developing PSO-ANFIS and GA-ANFIS models. To assess the optimum values of PSO, try and error technique was used resulted in acceptable values (Tables 2 and 3). Figs. 2 and 3 indicate the trained membership functions of the developed PSO-ANFIS and GA-ANFIS models, respectively. The structure of PSO-ANFIS model and its corresponding MFs are illustrated in Fig. 3. It

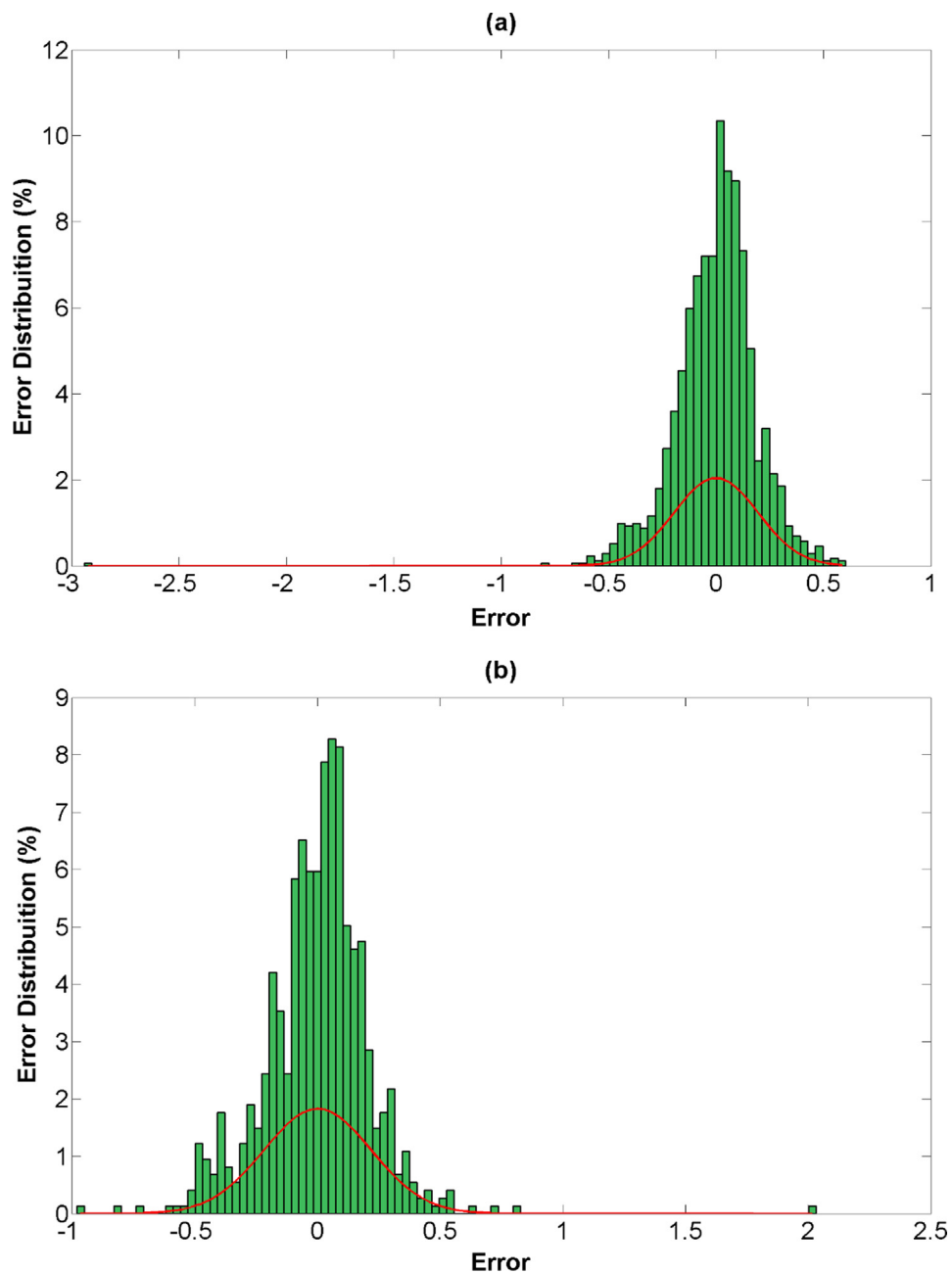


Fig. 8. Errors histogram for foreseeing the CO₂ solubility in various amines by RBF: (a) training dataset and (b) testing dataset.

indicates trained membership function parameters for input parameters, i.e. pressure, temperature, molarity, molecular weight, hydrogen bond donor count, hydrogen bond acceptor count, rotatable bond count and complexity for each cluster. The PSO-ANFIS and GA-ANFIS have 8 abovementioned inputs i.e., in1 to in8 and 10 clusters.

4.2. Model assessment

The comparative illustration of CO₂ absorption capacity, containing both experimental and model estimation values, for GA-ANFIS, PSO-ANFIS, RBF-ANN and LSSVM models are shown in Fig. 4. As can be seen, LSSVM method is capable to estimate experimental values of equilibrium CO₂ loading in different aqueous amine solvents with higher precision in comparison to the other models. Furthermore, the correlation plot between the results of different employed models (i.e., GA-ANFIS, PSO-ANFIS, RBF-ANN and LSSVM), as well as their experimentally obtained values for training and testing sets, are illustrated in

Fig. 5. The histogram of residual values (the difference between experimental and calculated values) was used as a demonstrative statistical technique to portray the model behavior (Figs. 6–9). Table 4 summarizes the statistical analyses of both experimental and model calculated CO₂ absorption in alkanolamine solvents. Based on the presented results, it is confirmed that the proposed LSSVM model is able to forecast the experiment data, better than other models with higher R² and lower MSE, STD, MAE and MRE values. Table 5 shows the R² and MRE values for CO₂ solubility estimation in 12 amine solutions using LSSVM model.

For the CO₂ solubility estimation by the LSSVM model, the R² of each amines is higher than 83% for almost all of the amines and LSSVM model could estimate the CO₂ solubility in DEAB with the highest R². Besides, MRE values for all of the amines are lower 0.15 except MDEA, DEA and DEEA. The models results indicate the accuracy of the proposed LSSVM models, exhibiting wide applicability in various amine solutions.

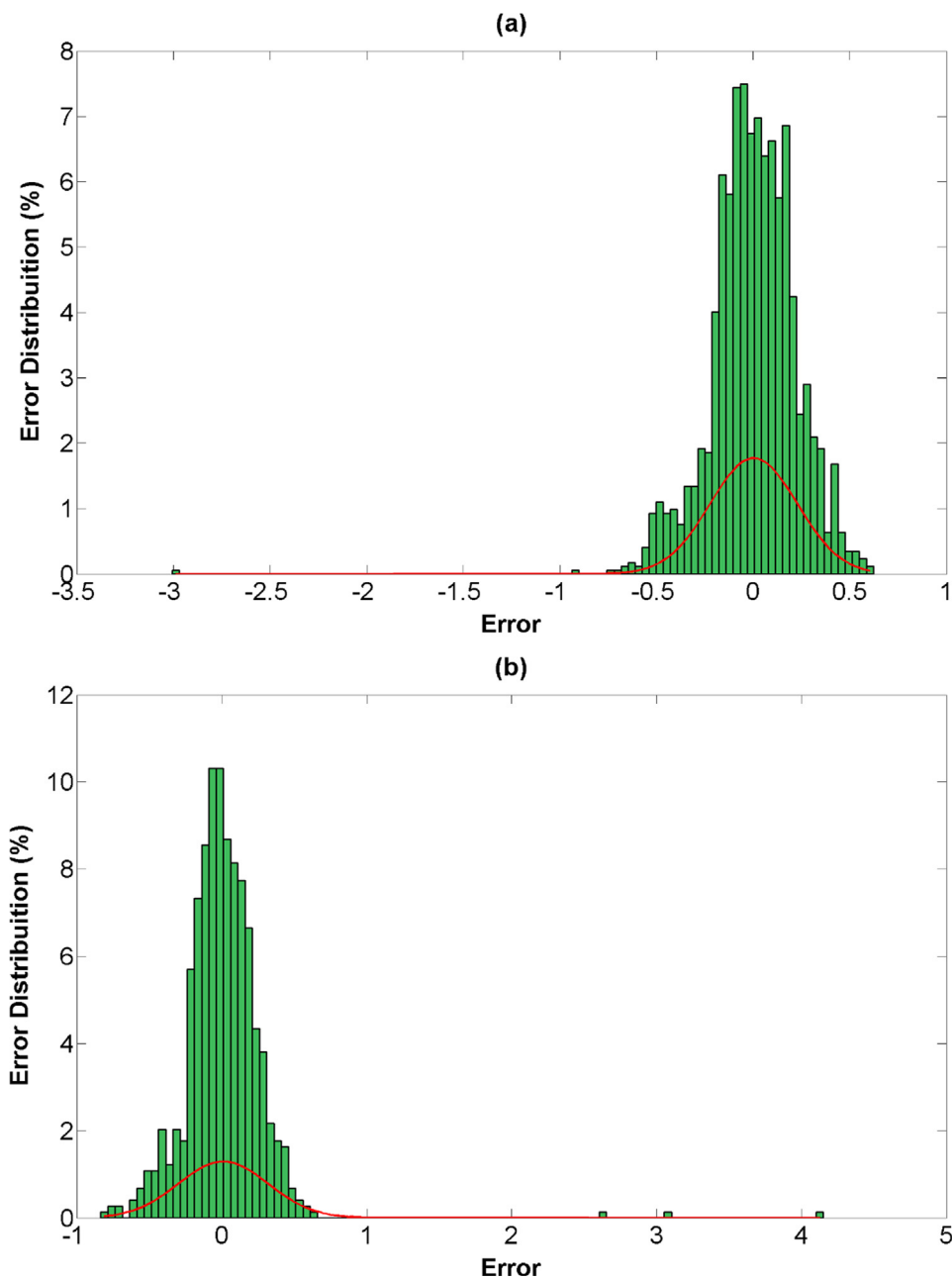


Fig. 9. Errors histogram for foreseeing the CO₂ solubility in various amines by GAANFIS: (a) training dataset and (b) testing dataset.

Table 4
Accuracy of the proposed models.

Model	RBF			LSSVM			PSO-ANFIS			GA-ANFIS			
	Dataset	Train	Test	Total	Train	Test	Total	Train	Test	Total	Train	Test	Total
R ²		0.9283	0.6338	0.8484	0.9441	0.9023	0.9338	0.8733	0.7942	0.8535	0.8311	0.6470	0.7760
MSE		0.0214	0.0929	0.0429	0.0167	0.0224	0.0184	0.0379	0.0474	0.0408	0.0506	0.0949	0.0639
MAE		0.0904	0.1514	0.1087	0.0788	0.1023	0.0858	0.1401	0.1557	0.1448	0.1673	0.1834	0.1722
STD		0.5270	0.4762	0.5124	0.5267	0.4527	0.5057	0.5111	0.4465	0.4927	0.5042	0.5035	0.5040
MRE		3.8216	2.9958	3.5733	1.9413	1.9352	1.9394	4.7257	2.8317	4.1562	9.1793	4.8671	7.8826

4.3. Outlier detection

As each model is validated by the experimental measurements, the authenticity of the model is highly affected by the accuracy of the used data points. As a result, a concept of outliers, known as the data points

separated from the overall trend, is defined [111]. To that end, in studies that utilize a large amount of data, it seems essential to discover rigorous approaches for detecting the outliers in order to improve the model accuracy by removing imprecise experimental data [112]. Herein, Leverage mathematical technique was employed as an outlier

Table 5

The R^2 and MRE values for CO_2 solubility estimation in 12 amine solutions using LSSVM model.

Type of Amine	DEEA	AMP	PZ	DEAB	MAE	MAPA	DEA	MEA	TIPA	MPA	MDEA	TEA
R^2	0.92	0.83	0.90	0.97	0.86	0.92	0.95	0.88	0.91	0.94	0.83	0.90
MRE	0.32	0.07	0.15	0.02	0.09	0.10	6.43	0.67	0.11	0.07	1.41	0.23

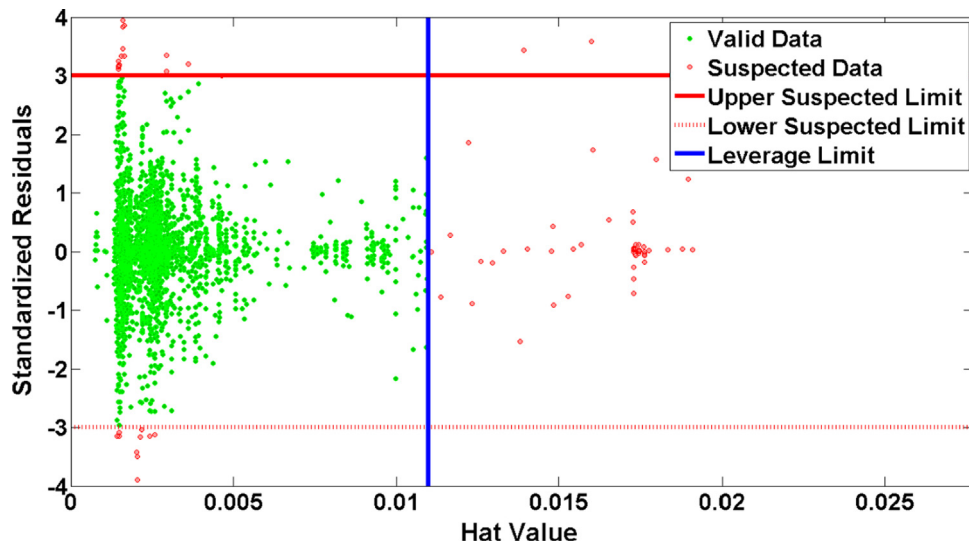


Fig. 10. Finding the likely suspected data for LSSVM model.

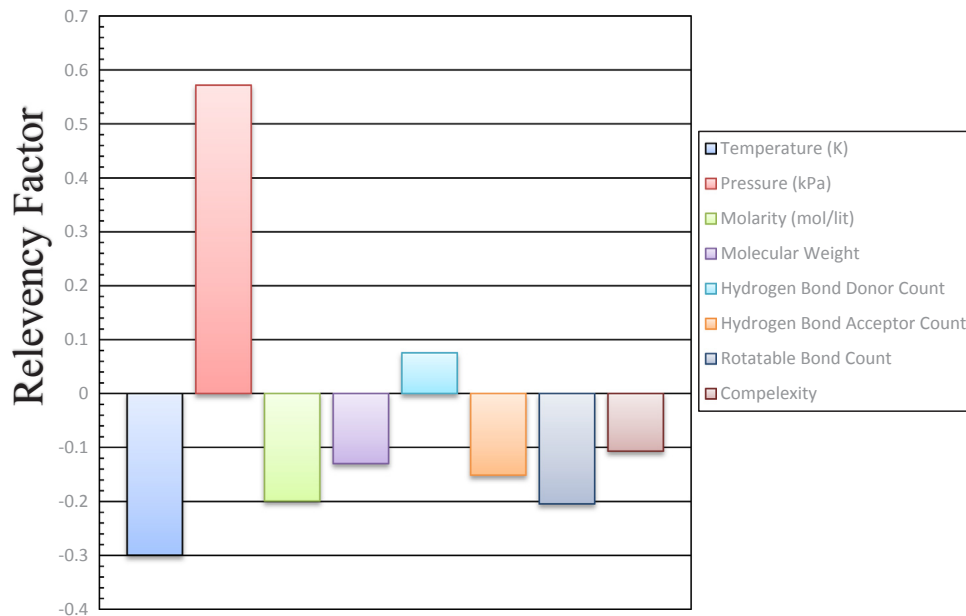


Fig. 11. Relative importance of input variables utilized to estimate CO_2 solubility in various Amines.

detection method. Throughout this approach, first the residual values are calculated. Then, according to the following formula, a Hat matrix of input data points is generated:

$$H = X(X^T X)^{-1} X^T \quad (32)$$

in which X represents the $m \times n$ matrix m and n symbolize the number of samples and model parameters, respectively. The hat amounts are achieved from the main diagonal of Hat matrix. On the other hand, William's plot is known as a graphical method for the outlier detection in which the standardized residuals are illustrated against the hat amounts. Within this study, considering the fact that the LVSSM model

has shown better predictive ability compared to the ANFIS, the outlier detection analysis of LVSSM has been presented. The William's plot of this model is indicated in Fig. 10. According to this plot, a critical leverage value (H^*) for the LVSSM model is obtained based on the following equation:

$$H^* = 3(n + 1)/m \quad (33)$$

In Fig. 10, the green line represents the leverage limit confirming that the data points with higher hat values (H) compared to the critical leverage value (H^*) are regarded as outliers. Additionally, based on the red lines signifying the limit boundaries which are $y = 3$ and $y = -3$,

the data points with higher standardized residuals than these lines can be considered as outliers. Accordingly, 54 of 2458 data points used in this study are outliers.

4.4. Sensitivity analysis

Sensitivity analysis is a method for finding the inputs effects on the outputs that is especially utilized for models through which a relationship between the inputs and outputs is made [113].

The LVSSM is presented to determine the most efficient inputs and their influence on the CO₂ loading capacity. For such as purpose, relevancy factor (r) equation method is employed in which the amount of (r) varies between -1 and +1. In this method, higher absolute value of r for an input and output indicates that the input can affect the output to a larger extent. A positive value of the coefficient specifies that the output increases by an increase in the input whereas a negative coefficient indicates that the output decreases with an increase in the input. The amount of r can be determined as follows [112]:

$$r = \frac{\sum_{i=1}^n (X_{k,i} - \bar{X}_k)(Y_i - \bar{Y})}{\sqrt{\sum_{i=1}^n (X_{k,i} - \bar{X}_k)^2 \sum_{i=1}^n (Y_i - \bar{Y})^2}} \quad (34)$$

where X_{k,i}, \bar{X}_k , Y_i, \bar{Y} and n represent the 'i'th input value, the average value of the k'th input, the 'i'th output value, the average value of output and the number data sets, respectively. Eventually, according to Fig. 11, it can be concluded that there is a direct relationship between the CO₂ loading capacity and the pressure and hydrogen bond donor count while the average molecular weight, hydrogen bond acceptor count, rotatable bond count complexity of the amines, molarity and temperature have inverse relationships with the CO₂ loading capacity. In addition, the pressure has the highest impact on CO₂ loading capacity with the r factor of 0.57 followed by the temperature with 0.29. Finally, the hydrogen bond donor count can be considered the least effective input feature with 0.07.

5. Conclusion

In this work, different models (i.e. GA-ANFIS, PSO-ANFIS, RBF-ANN and LSSVM) were successfully developed to anticipate the equilibrium absorption capacity of CO₂ in 12 aqueous alkanolamine solutions. The results indicate that the models are capable to acceptably estimate experimental values of CO₂ loading over a wide range of independent variables (i.e. CO₂ partial pressure, temperature and amine concentration). Furthermore, it is declared that the results of the developed model (in this study) are in good agreement with experimental results with higher accuracy and better performance. The results also indicate that LSSVM acceptably estimates experimental values with R² of 0.93. However, the results of LSSVM model are more promising for most of the aqueous amine solvents.

Appendix A. Supplementary data

Supplementary data to this article can be found online at <https://doi.org/10.1016/j.fuel.2019.116616>.

References

- [1] Ghiasi MM, Arabloo M, Mohammadi AH, Barghi T. Application of ANFIS soft computing technique in modeling the CO₂ capture with MEA, DEA, and TEA aqueous solutions. *Int J Greenhouse Gas Control* 2016;49:47–54.
- [2] Dashti A, Raji M, Azarafza A, Baghban A, Mohammadi AH, Asghari M. Rigorous prognostication and modeling of gas adsorption on activated carbon and Zeolite-5A. *J Environ Manage* 2018;224:58–68.
- [3] Dashti A, Raji M, Razmi A, Rezaei N, Zendehboudi S, Asghari M. Efficient hybrid modeling of CO₂ absorption in aqueous solution of piperazine: applications to energy and environment. *Chem Eng Res Des* 2019.
- [4] Rochelle GT. Amine scrubbing for CO₂ capture. *Science* 2009;325(5948):1652–4.
- [5] Zhang S, Lu Y. Surfactants facilitating carbonic anhydrase enzyme-mediated CO₂ absorption into a carbonate solution. *Environ Sci Technol* 2017;51(15):8537–43.
- [6] Yousef AM, El-Maghly WM, Eldrainy YA, Attia A. New approach for biogas purification using cryogenic separation and distillation process for CO₂ capture. *Energy* 2018;156:328–51.
- [7] Samanta A, Zhao A, Shimizu GK, Sarkar P, Gupta R. Post-combustion CO₂ capture using solid sorbents: a review. *Ind Eng Chem Res* 2011;51(4):1438–63.
- [8] Sodeifian G, Raji M, Asghari M, Rezakazemi M, Dashti A. Polyurethane-SAPO-34 mixed matrix membrane for CO₂/CH₄ and CO₂/N₂ separation. *Chin J Chem Eng* 2018.
- [9] Paul DR. Polymeric gas separation membranes. CRC Press; 2018.
- [10] Castel C, Wang L, Corriu JP, Favre E. Steady vs unsteady membrane gas separation processes. *Chem Eng Sci* 2018;183:136–47.
- [11] Rufford TE, Smart S, Watson GC, Graham B, Boxall J, Da Costa JD, et al. The removal of CO₂ and N₂ from natural gas: a review of conventional and emerging process technologies. *J Petrol Sci Eng* 2012;94:123–54.
- [12] Herslund PJ, Thomsen K, Abildskov J, von Solms N. Phase equilibrium modeling of gas hydrate systems for CO₂ capture. *J Chem Thermodyn* 2012;48:13–27.
- [13] Vaidya PD, Kenig EY. CO₂-alkanolamine reaction kinetics: a review of recent studies. *Chem Eng Technol* 2007;30(11):1467–74.
- [14] Liu F, Fang M, Dong W, Wang T, Xia Z, Wang Q, et al. Carbon dioxide absorption in aqueous alkanolamine blends for biphasic solvents screening and evaluation. *Appl Energy* 2019;233:468–77.
- [15] Conway W, Bruggink S, Beyad Y, Luo W, Melián-Cabrera I, Puxty G, et al. CO₂ absorption into aqueous amine blended solutions containing monoethanolamine (MEA), N, N-dimethylethanolamine (DMEA), N, N-diethylethanolamine (DEEA) and 2-amino-2-methyl-1-propanol (AMP) for post-combustion capture processes. *Chem Eng Sci* 2015;126:446–54.
- [16] Ling H, Gao H, Liang Z. Comprehensive solubility of N₂O and mass transfer studies on an effective reactive N, N-dimethylethanolamine (DMEA) solvent for post-combustion CO₂ capture. *Chem Eng J* 2019;355:369–79.
- [17] Fouad WA, Berrouk AS. Prediction of H₂S and CO₂ solubilities in aqueous triethanolamine solutions using a simple model of Kent-Eisenberg type. *Ind Eng Chem Res* 2012;51(18):6591–7.
- [18] Garg S, Shariff A, Shaikh M, Lal B, Aftab A, Faiqa N. VLE of CO₂ in aqueous potassium salt of L-phenylalanine: experimental data and modeling using modified Kent-Eisenberg model. *J Nat Gas Sci Eng* 2016;34:864–72.
- [19] Chen CC, Evans LB. A local composition model for the excess Gibbs energy of aqueous electrolyte systems. *AIChE J* 1986;32(3):444–54.
- [20] Deshmukh R, Mather A. A mathematical model for equilibrium solubility of hydrogen sulfide and carbon dioxide in aqueous alkanolamine solutions. *Chem Eng Sci* 1981;36(2):355–62.
- [21] Haqitalab A, Dehghani Tafti M. Electrolyte UNIQUAC – NRF model to study the solubility of acid gases in alkanolamines. *Ind Eng Chem Res* 2007;46(18):6053–60.
- [22] Aronu UE, Gondal S, Hessen ET, Haug-Warberg T, Hartono A, Hoff KA, et al. Solubility of CO₂ in 15, 30, 45 and 60 mass% MEA from 40 to 120 °C and model representation using the extended UNIQUAC framework. *Chem Eng Sci* 2011;66(24):6393–406.
- [23] Benamor A, Aroua M. Modeling of CO₂ solubility and carbamate concentration in DEA, MDEA and their mixtures using the Deshmukh-Mather model. *Fluid Phase Equilib* 2005;231(2):150–62.
- [24] Saghafi H, Arabloo M. Modeling of CO₂ solubility in MEA, DEA, TEA, and MDEA aqueous solutions using AdaBoost-decision tree and artificial neural network. *Int J Greenhouse Gas Control* 2017;58:256–65.
- [25] Rezakazemi M, Azarafza A, Dashti A, Shirazian S. Development of hybrid models for prediction of gas permeation through FS/POSS/PDMS nanocomposite membranes. *Int J Hydrogen Energy* 2018;43(36):17283–94.
- [26] Dashti A, Harami HR, Rezakazemi M, Shirazian S. Estimating CH₄ and CO₂ solubilities in ionic liquids using computational intelligence approaches. *J Mol Liq* 2018;271:661–9.
- [27] Salooki MK, Abedini R, Adib H, Koolivand H. Design of neural network for manipulating gas refinery sweetening regenerator column outputs. *Sep Purif Technol* 2011;82:1–9.
- [28] Adib H, Sharifi F, Mehranbod N, Kazerooni NM, Koolivand M. Support Vector Machine based modeling of an industrial natural gas sweetening plant. *J Nat Gas Sci Eng* 2013;14:121–31.
- [29] Ghiasi MM, Mohammadi AH. Rigorous modeling of CO₂ equilibrium absorption in MEA, DEA, and TEA aqueous solutions. *J Nat Gas Sci Eng* 2014;18:39–46.
- [30] Saghatoslimi N, Salooki M, Mohamadi N. Auto-design of neural network-based GAS for manipulating the khangiran gas refinery sweetening absorption column outputs. *Pet Sci Technol* 2011;29(14):1437–48.
- [31] Sipöcz N, Tobiesen FA, Assadi M. The use of Artificial Neural Network models for CO₂ capture plants. *Appl Energy* 2011;88(7):2368–76.
- [32] Zhou Q, Wu Y, Chan CW, Tontiwachwuthikul P. From neural network to neuro-fuzzy modeling: applications to the carbon dioxide capture process. *Energy Proc* 2011;4:2066–73.
- [33] Zhou Q, Chan C, Tontiwachwuthikul P, Idem R, Gelowitz D. Application of neuro-fuzzy modeling technique for operational problem solving in a CO₂ capture process system. *Int J Greenhouse Gas Control* 2013;15:32–41.
- [34] Zhou Q, Wu Y, Chan CW, Tontiwachwuthikul P. Modeling of the carbon dioxide capture process system using machine intelligence approaches. *Eng Appl Artif Intell* 2011;24(4):673–85.
- [35] Wu Y, Chan CW. Analysis of data for the carbon dioxide capture domain. *Eng Appl Artif Intell* 2011;24(1):154–63.
- [36] Daneshvar N, Moattar MZ, Abdi MA, Aber S. Carbon dioxide equilibrium absorption in the multi-component systems of CO₂+ TIPA+ MEA+ H₂O, CO₂+ TIPA+ Pz+ H₂O and CO₂+ TIPA+ H₂O at low CO₂ partial pressures:

- experimental solubility data, corrosion study and modeling with artificial neural network. *Sep Purif Technol* 2004;37(2):135–47.
- [37] Shahsavand A, Fard FD, Sotoudeh F. Application of artificial neural networks for simulation of experimental CO₂ absorption data in a packed column. *J Nat Gas Sci Eng* 2011;3(3):518–29.
- [38] Pahlavanzadeh H, Nourani S, Saber M. Experimental analysis and modeling of CO₂ solubility in AMP (2-amino-2-methyl-1-propanol) at low CO₂ partial pressure using the models of Deshmukh-Mather and the artificial neural network. *J Chem Thermodyn* 2011;43(12):1775–83.
- [39] ZareNezhad B, Aminian A. An artificial neural network model for predicting the H₂S removal performance of piperazine solvents in gas sweetening plants. *J Univ Chem Technol Metall* 2012;47(5).
- [40] ZareNezhad B, Aminian A. A neuro-fuzzy model for accurate prediction of H₂S solubilities in aqueous solvents employed in water-wash units of gas refining plants. *J Univ Chem Technol Metall* 2012;47(5).
- [41] Bastani D, Hamzehie M, Davardoost F, Mazinani S, Poorbashiri A. Prediction of CO₂ loading capacity of chemical absorbents using a multi-layer perceptron neural network. *Fluid Phase Equilib* 2013;354:6–11.
- [42] Yu H, Xie T, Paszcynski S, Wilamowski BM. Advantages of radial basis function networks for dynamic system design. *IEEE Trans Ind Electron* 2011;58(12):5438–50.
- [43] Lee KH. Application of a radial basis function neural network to estimate pressure gradient in water-oil pipelines. First Course on Fuzzy Theory Appl. 2005.
- [44] Broomhead DS, Lowe D. Radial basis functions, multi-variable functional interpolation and adaptive networks. Royal Signals and Radar Establishment Malvern (United Kingdom). 1988.
- [45] Seshagiri S, Khalil HK. Output feedback control of nonlinear systems using RBF neural networks. *IEEE Trans Neural Networks* 2000;11(1):69–79.
- [46] Lotfi IA. Modeling discharge-suspended sediment relationship using least square support vector machine. *Inf. Control* 1965;8(3):338–53.
- [47] Khajeh A, Modarress H. Prediction of solubility of gases in polystyrene by adaptive neuro-fuzzy inference system and radial basis function neural network. *Expert Syst Appl* 2010;37(4):3070–4.
- [48] Eberhart R, Kennedy J. A new optimizer using particle swarm theory. Micro machine and human science, 1995. MHS'95. Proceedings of the Sixth International Symposium on. IEEE. 1995. p. 39–43.
- [49] Panigrahi BK, Shi Y, Lim M-H. Handbook of swarm intelligence: concepts, principles and applications. Springer Science & Business Media; 2011.
- [50] Sharma A, Onwubolu G. Hybrid particle swarm optimization and GMDH system. Hybrid Self-Organizing Modeling Systems. Springer; 2009. p. 193–231.
- [51] Castillo O. Introduction to type-2 fuzzy logic control. Type-2 fuzzy logic in intelligent control applications. Springer; 2012. p. 3–5.
- [52] Onwunalu JE, Durlofsky LJ. Application of a particle swarm optimization algorithm for determining optimum well location and type. *Comput Geosci* 2010;14(1):183–98.
- [53] Chen M-Y. A hybrid ANFIS model for business failure prediction utilizing particle swarm optimization and subtractive clustering. *Inf Sci* 2013;220:180–95.
- [54] Lin C-J, Hong S-J. The design of neuro-fuzzy networks using particle swarm optimization and recursive singular value decomposition. *Neurocomputing* 2007;71(1–3):297–310.
- [55] Shi Y, Eberhart R. A modified particle swarm optimizer. Evolutionary Computation Proceedings, 1998. IEEE World Congress on Computational Intelligence, The 1998 IEEE International Conference on. IEEE. 1998. p. 69–73.
- [56] Chiou J-S, Tsai S-H, Liu M-T. A PSO-based adaptive fuzzy PID-controllers. *Simul Model Pract Theory* 2012;26:49–59.
- [57] Karkevandi-Talkhooncheh A, Hajirezaie S, Hemmati-Sarapardeh A, Husein MM, Karan K, Sharifi M. Application of adaptive neuro fuzzy interface system optimized with evolutionary algorithms for modeling CO₂-crude oil minimum miscibility pressure. *Fuel* 2017;205:34–45.
- [58] Suykens JA, Vandewalle J. Least squares support vector machine classifiers. *Neural Process Lett* 1999;9(3):293–300.
- [59] Cortes C, Vapnik V. Support-vector networks. *Mach Learn* 1995;20(3):273–97.
- [60] Amendolia SR, Cossu G, Ganadu M, Golosio B, Masala G, Mura GM. A comparative study of k-nearest neighbour, support vector machine and multi-layer perceptron for thalassemia screening. *Chemometr Intell Lab Syst* 2003;69(1–2):13–20.
- [61] Shokrollahi A, Tatar A, Safari H. On accurate determination of PVT properties in crude oil systems: committee machine intelligent system modeling approach. *J Taiwan Inst Chem Eng* 2015;55:17–26.
- [62] Rafiee-Taghanaki S, Arabloo M, Chamkalan A, Amani M, Zargari MH, Adelzadeh MR. Implementation of SVM framework to estimate PVT properties of reservoir oil. *Fluid Phase Equilib* 2013;346:25–32.
- [63] Baylar A, Hanbay D, Batan M. Application of least square support vector machines in the prediction of aeration performance of plunging overfall jets from weirs. *Expert Syst Appl* 2009;36(4):8368–74.
- [64] Suykens JA, Vandewalle J. Multiclass least squares support vector machines. Proceedings of the international joint conference on neural networks. 1999. p. 900–3.
- [65] Suykens JA, Van Gestel T, De Brabanter J. Least squares support vector machines. World Scientific; 2002.
- [66] Suykens JA, Vandewalle J, De Moor B. Intelligence and cooperative search by coupled local minimizers. *Int J Bifurcation Chaos* 2001;11(08):2133–44.
- [67] Gunn SR. Support vector machines for classification and regression. *ISIS Tech Rep* 1998;14(1):5–16.
- [68] Muller K-R, Mika S, Ratsch G, Tsuda K, Scholkopf B. An introduction to kernel-based learning algorithms. *IEEE Trans Neural Networks* 2001;12(2):181–201.
- [69] Hemmati-Sarapardeh A, Varamesh A, Husein MM, Karan K. On the evaluation of the viscosity of nanofluid systems: modeling and data assessment. *Renew Sustain Energy Rev* 2018;81:313–29.
- [70] Xavier-de-Souza S, Suykens JA, Vandewalle J, Bollé D. Coupled simulated annealing. *IEEE Trans Syst Man Cyber B (Cybernetics)* 2010;40(2):320–35.
- [71] Kundu M, Mandal BP, Bandyopadhyay SS. Vapor – liquid equilibrium of CO₂ in aqueous solutions of 2-amino-2-methyl-1-propanol. *J Chem Eng Data* 2003;48(4):789–96.
- [72] Dash SK, Samanta A, Samanta AN, Bandyopadhyay SS. Vapour liquid equilibria of carbon dioxide in dilute and concentrated aqueous solutions of piperazine at low to high pressure. *Fluid Phase Equilib* 2011;300(1):145–54.
- [73] Derk P, Dijkstra H, Hogendoorn J, Versteeg G. Solubility of carbon dioxide in aqueous piperazine solutions. *AIChE J* 2005;51(8):2311–27.
- [74] Bishnoi S, Rochelle GT. Absorption of carbon dioxide into aqueous piperazine: reaction kinetics, mass transfer and solubility. *Chem Eng Sci* 2000;55(22):5531–43.
- [75] Park J-Y, Yoon SJ, Lee H, Yoon J-H, Shim J-G, Lee JK, et al. Solubility of carbon dioxide in aqueous solutions of 2-amino-2-ethyl-1, 3-propanediol. *Fluid Phase Equilib* 2002;202(2):359–66.
- [76] Gabrielsen J, Michelsen ML, Stenby EH, Kontogeorgis GM. A model for estimating CO₂ solubility in aqueous alkanolamines. *Ind Eng Chem Res* 2005;44(9):3348–54.
- [77] Ma'mun S, Nilsen R, Svendsen HF, Juliussen O. Solubility of carbon dioxide in 30 mass% monoethanolamine and 50 mass% methylidiethanolamine solutions. *J Chem Eng Data* 2005;50(2):630–4.
- [78] Park SH, Lee KB, Hyun JC, Kim SH. Correlation and prediction of the solubility of carbon dioxide in aqueous alkanolamine and mixed alkanolamine solutions. *Ind Eng Chem Res* 2002;41(6):1658–65.
- [79] Porcheron F, Gibert A, Mougin P, Wender A. High throughput screening of CO₂ solubility in aqueous monoamine solutions. *Environ Sci Technol* 2011;45(6):2486–92.
- [80] Jou FY, Mather AE, Otto FD. The solubility of CO₂ in a 30 mass percent monoethanolamine solution. *Canad J Chem Eng* 1995;73(1):140–7.
- [81] Jane I-S, Li M-H. Solubilities of mixtures of carbon dioxide and hydrogen sulfide in water + diethanolamine + 2-amino-2-methyl-1-propanol. *J Chem Eng Data* 1997;42(1):98–105.
- [82] Jones J, Froning H, Clayton Jr E. Solubility of acidic gases in aqueous monoethanolamine. *J Chem Eng Data* 1959;4(1):85–92.
- [83] Lee J, Otto F, Mather A. The solubility of mixtures of carbon dioxide and hydrogen sulphide in aqueous diethanolamine solutions. *Canad J Chem Eng* 1974;52(1):125–7.
- [84] Isaacs EE, Otto FD, Mather AE. Solubility of mixtures of hydrogen sulfide and carbon dioxide in a monoethanolamine solution at low partial pressures. *J Chem Eng Data* 1980;25(2):118–20.
- [85] Lee JI, Otto FD, Mather AE. Equilibrium between carbon dioxide and aqueous monoethanolamine solutions. *J Appl Chem Biotech* 1976;26(1):541–9.
- [86] Shen KP, Li MH. Solubility of carbon dioxide in aqueous mixtures of monoethanolamine with methylidiethanolamine. *J Chem Eng Data* 1992;37(1):96–100.
- [87] Rho S-W, Yoo K-P, Lee JS, Nam SC, Son JE, Min B-M. Solubility of CO₂ in aqueous methylidiethanolamine solutions. *J Chem Eng Data* 1997;42(6):1161–4.
- [88] Maddox R, Bhairi A, Diers JR, Thomas P. Equilibrium solubility of carbon dioxide or hydrogen sulfide in aqueous solutions of monoethanolamine, diglycolamine, diethanolamine and methylidiethanolamine: project 841. Gas Processors Association; 1987.
- [89] Lemoine B, Li Y-G, Cadours R, Bouallou C, Richon D. Partial vapor pressure of CO₂ and H₂S over aqueous methylidiethanolamine solutions. *Fluid Phase Equilib* 2000;172(2):261–77.
- [90] Sidi-Boumedine R, Horstmann S, Fischer K, Provost E, Fürst W, Gmehling J. Experimental determination of carbon dioxide solubility data in aqueous alkanolamine solutions. *Fluid Phase Equilib* 2004;218(1):85–94.
- [91] Huttonhuus PJG, Agrawal N, Hogendoorn J, Versteeg G. Gas solubility of H₂S and CO₂ in aqueous solutions of N-methylidiethanolamine. *J Petrol Sci Eng* 2007;55(1–2):122–34.
- [92] Park MK, Sandall OC. Solubility of carbon dioxide and nitrous oxide in 50 mass methylidiethanolamine. *J Chem Eng Data* 2001;46(1):166–8.
- [93] Haji-Sulaiman M, Aroua M, Benamor A. Analysis of equilibrium data of CO₂ in aqueous solutions of diethanolamine (DEA), methylidiethanolamine (MDEA) and their mixtures using the modified Kent Eisenberg model. *Chem Eng Res Des* 1998;76(8):961–8.
- [94] Aroua M, Haji-Sulaiman M, Ramasamy K. Modelling of carbon dioxide absorption in aqueous solutions of AMP and MDEA and their blends using Aspenplus. *Sep Purif Technol* 2002;29(2):153–62.
- [95] Xu G-W, Zhang C-F, Qin S-J, Gao W-H, Liu H-B. Gas – liquid equilibrium in a CO₂ – MDEA – H₂O system and the effect of piperazine on it. *Ind Eng Chem Res* 1998;37(4):1473–7.
- [96] Bishnoi S, Rochelle GT. Thermodynamics of piperazine/methylidiethanolamine/water/carbon dioxide. *Ind Eng Chem Res* 2002;41(3):604–12.
- [97] Lee JI, Otto FD, Mather AE. Solubility of carbon dioxide in aqueous diethanolamine solutions at high pressures. *J Chem Eng Data* 1972;17(4):465–8.
- [98] Lee JI, Otto FD, Mather AE. Solubility of hydrogen sulfide in aqueous diethanolamine solutions at high pressures. *J Chem Eng Data* 1973;18(1):71–3.
- [99] Vallée G, Mougin P, Julian S, Fürst W. Representation of CO₂ and H₂S absorption by aqueous solutions of diethanolamine using an electrolyte equation of state. *Ind*

- Eng Chem Res 1999;38(9):3473–80.
- [105] Mason JW, Dodge BF. Equilibrium absorption of carbon dioxide by solutions of the ethanolamines. *Trans Am Inst Chem Eng* 1936;32:27–48.
- [106] Chung P-Y, Soriano AN, Leron RB, Li M-H. Equilibrium solubility of carbon dioxide in the amine solvent system of (triethanolamine + piperazine + water). *J Chem Thermodyn* 2010;42(6):802–7.
- [107] Sema T, Naami A, Idem R, Tontiwachwuthikul P. Correlations for equilibrium solubility of carbon dioxide in aqueous 4-(diethylamino)-2-butanol solutions. *Ind Eng Chem Res* 2011;50(24):14008–15.
- [108] Arshad MW, Svendsen HF, Fosbøl PL, von Solms N, Thomsen K. Equilibrium total pressure and CO₂ solubility in binary and ternary aqueous solutions of 2-(diethylamino) ethanol (DEEA) and 3-(methylamino) propylamine (MAPA). *J Chem Eng Data* 2014;59(3):764–74.
- [109] Kumar G, Kundu M. Vapour–liquid equilibrium of CO₂ in aqueous solutions of N-methyl-2-ethanolamine. *Canad J Chem Eng* 2012;90(3):627–30.
- [110] Dong L, Chen J, Gao G. Solubility of carbon dioxide in aqueous solutions of 3-amino-1-propanol. *J Chem Eng Data* 2009;55(2):1030–4.
- [111] Rousseeuw PJ, Leroy AM. Robust regression and outlier detection. John Wiley & Sons; 2005. p. 3–6.
- [112] Hosseini zadeh M, Hemmati-Sarapardeh A. Toward a predictive model for estimating viscosity of ternary mixtures containing ionic liquids. *J Mol Liq* 2014;200:340–8.
- [113] Raji M, Dashti A, Amani P, Mohammadi AH. Efficient estimation of CO₂ solubility in aqueous salt solutions. *J Mol Liq* 2019. In press.
- [114] Jang J-SR. ANFIS: adaptive-network-based fuzzy inference system. *IEEE Trans Syst. Man Cybern.* 1993;23.
- [115] Onwunalu JE, Durlofsky LJ. Application of a particle swarm optimization algorithm for determining optimum well location and type. *Comput. Geosci.* 2010;14:183–98.